Fundamentals of synchronization in chaotic systems, concepts, and applications

Louis M. Pecora, Thomas L. Carroll, Gregg A. Johnson, and Douglas J. Mar
Code 6343, U.S. Naval Research Laboratory, Washington, District of Columbia 20375

James F. Heagy
Institutes for Defense Analysis, Science and Technology Division, Alexandria, Virginia 22311-1772

(Received 29 April 1997; accepted for publication 29 September 1997)

The field of chaotic synchronization has grown considerably since its advent in 1990. Several subdisciplines and ''cottage industries'' have emerged that have taken on *bona fide* lives of their own. Our purpose in this paper is to collect results from these various areas in a review article format with a tutorial emphasis. Fundamentals of chaotic synchronization are reviewed first with emphases on the geometry of synchronization and stability criteria. Several widely used coupling configurations are examined and, when available, experimental demonstrations of their success (generally with chaotic circuit systems) are described. Particular focus is given to the recent notion of synchronous substitution—a method to synchronize chaotic systems using a larger class of scalar chaotic coupling signals than previously thought possible. Connections between this technique and well-known control theory results are also outlined. Extensions of the technique are presented that allow so-called hyperchaotic systems (systems with more than one positive Lyapunov exponent) to be synchronized. Several proposals for ''secure'' communication schemes have been advanced; major ones are reviewed and their strengths and weaknesses are touched upon. Arrays of coupled chaotic systems have received a great deal of attention lately and have spawned a host of interesting and, in some cases, counterintuitive phenomena including bursting above synchronization thresholds, destabilizing transitions as coupling increases (short-wavelength bifurcations), and riddled basins. In addition, a general mathematical framework for analyzing the stability of arrays with arbitrary coupling configurations is outlined. Finally, the topic of generalized synchronization is discussed, along with data analysis techniques that can be used to decide whether two systems satisfy the mathematical requirements of generalized synchronization. [S1054-1500(97)02904-2]

Since the early 1990s researchers have realized that chaotic systems can be synchronized. The recognized potential for communications systems has driven this phenomenon to become a distinct subfield of nonlinear dynamics, with the need to understand the phenomenon in its most fundamental form viewed as being essential. All forms of identical synchronization, where two or more dynamical system execute the same behavior at the same time, are really manifestations of dynamical behavior restricted to a flat hyperplane in the phase space. This is true whether the behavior is chaotic, periodic, fixed point, etc. This leads to two fundamental considerations in studying synchronization: (1) finding the hyperplane and (2) determining its stability. Number (2) is accomplished by determining whether perturbations transverse to the hyperplane damp out or are amplified. If they damp out, the motion is restricted to the hyperplane and the synchronized state is stable. Because the fundamental geometric requirement of an invariant hyperplane is so simple, many different types of synchronization schemes are possible in both unidirectional and bidirectional coupling scenarios. Many bidirectional cases display behavior that is counterintuitive: increasing coupling strength can destroy the synchronous state, the simple Lyapunov exponent threshold is not necessarily the most practical, and basins of attraction for synchronous attractors are not necessarily simple, leading to fundamental problems in predicting the final state of the whole dynamical system. Finally, detecting synchronization and related phenomena from a time series is not a trivial problem and requires the invention of new statistics that gauge the mathematical relations between attractors reconstructed from two times series, such as continuity and differentiability.

I. INTRODUCTION: CHAOTIC SYSTEMS CAN SYNCHRONIZE

Chaos has long-term unpredictable behavior. This is usually couched mathematically as a sensitivity to initial conditions—where the system's dynamics takes it is hard to predict from the starting point. Although a chaotic system can have a pattern (an attractor) in state space, determining where on the attractor the system is at a distant, future time given its position in the past is a problem that becomes exponentially harder as time passes. One way to demonstrate this is to run two, identical chaotic systems side by side, starting both at close, but not exactly equal initial conditions.

The systems soon diverge from each other, but both retain the same attractor pattern. Where each is on its own attractor has no relation to where the other system is.

An interesting question to ask is, can we force the two chaotic systems to follow the same path on the attractor? Perhaps we could ''lock'' one to the other and thereby cause their synchronization? The answer is, yes.

Why would we want to do this? The noise-like behavior of chaotic systems suggested early on that such behavior might be useful in some type of private communications. One glance at the Fourier spectrum from a chaotic system will suggest the same. There are typically no dominant peaks, no special frequencies. The spectrum is broadband.

To use a chaotic signal in communications we are immediately led to the requirement that somehow the receiver must have a duplicate of the transmitter's chaotic signal or, better yet, synchronize with the transmitter. In fact, synchronization is a requirement of many types of communication systems, not only chaotic ones. Unfortunately, if we look at how other signals are synchronized we will get very little insight as to how to do it with chaos. New methods are therefore required.

There have been suggestions to use chaos in robotics or biological implants. If we have several parts that we would like to act together, although chaotically, we are again led to the synchronization of chaos. For simplicity we would like to be able to achieve such synchronization using a minimal number of signals between the synchronous parts, one signal passed among them would be best.

In spatiotemporal systems we are often faced with the study of the transition from spatially uniform motion to spatially varying motion, perhaps even spatially chaotic. For example, the Belousov–Zhabotinskii chemical reaction can be chaotic, but spatially uniform in a well-stirred experiment.[1] This means that all spatial sites are synchronized with each other—they are all doing the same thing at the same time, even if it is chaotic motion. But in other circumstances the uniformity can become unstable and spatial variations can surface. Such uniform to nonuniform bifurcations are common in spatiotemporal systems. How do such transitions occur? What are the characteristics of these bifurcations? We are asking physical and dynamical questions regarding synchronized, chaotic states.

Early work on synchronous, coupled chaotic systems was done by Yamada and Fujisaka.[2,3] In that work, some sense of how the dynamics might change was brought out by a study of the Lyapunov exponents of synchronized, coupled systems. Although Yamada and Fujisaka were the first to exploit local analysis for the study of synchronized chaos, their papers went relatively unnoticed. Later, a now-famous paper by Afraimovich, Verichev, and Rabinovich[4] exposed many of the concepts necessary for analyzing synchronous chaos, although it was not until many years later that widespread study of synchronized, chaotic systems took hold. We build on the early work and our own studies[5–10] to develop a geometric view of this behavior.

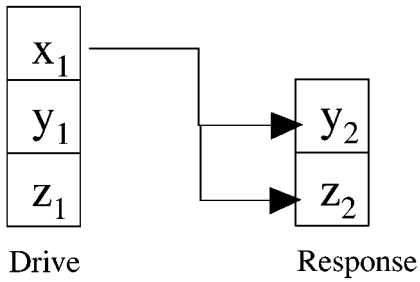

FIG. 1. Original drive–response scheme for complete replacement synchronization.

II. GEOMETRY: SYNCHRONIZATION HYPERPLANES

A. Simple example

Let us look at a simple example. Suppose we start with two Lorenz chaotic systems. Then we transmit a signal from the first to the second. Let this signal be the x component of the first system. In the second system everywhere we see an x component we replace it with the signal from the first system. We call this construction *complete replacement*. This gives us a new five dimensional compound system:

$$\frac{dx_1}{dt} = -\sigma(y_1 - x_1),$$

$$\frac{dy_1}{dt} = -x_1 z_1 + r x_1 - y_1, \quad \frac{dy_2}{dt} = -x_1 z_2 + r x_1 - y_2, \quad (1)$$

$$\frac{dz_1}{dt} = x_1 y_1 - b z_1, \quad \frac{dz_2}{dt} = x_1 y_2 - b z_2,$$

where we have used subscripts to label each system. Note that we have replaced x_2 by x_1 in the second set of equations and eliminated the $\dot{x}_1$ equation, since it is superfluous. We can think of the x_1 variable as driving the second system. Figure 1 shows this setup schematically. We use this view to label the first system the *drive* and the second system the *response*. If we start Eq. (1) from arbitrary initial conditions we will soon see that y_2 converges to y_1 and z_2 converges to z_1 as the systems evolve. After long times the motion causes the two equalities $y_2 = y_1$ and $z_2 = z_1$. The y and z components of both systems stay equal to each other as the system evolves. We now have a set of synchronized, chaotic systems. We refer to this situation as *identical synchronization* since both (y,z) subsystems are identical, which manifests in the equality of the components.

We can get an idea of what the geometry of the synchronous attractor looks like in phase space using the above example. We plot the variables x_1, y_1, and y_2. Since $y_2 = y_1$ we see that the motion remains on the plane defined by this equality. Similarly, the motion must remain on the plane defined by $z_2 = z_1$. Such equalities define a hyperplane in the five-dimensional state space. We see a projection of this (in three dimensions) in Fig. 2. The constraint of motion to a hyperplane and the existence of identical synchronization are

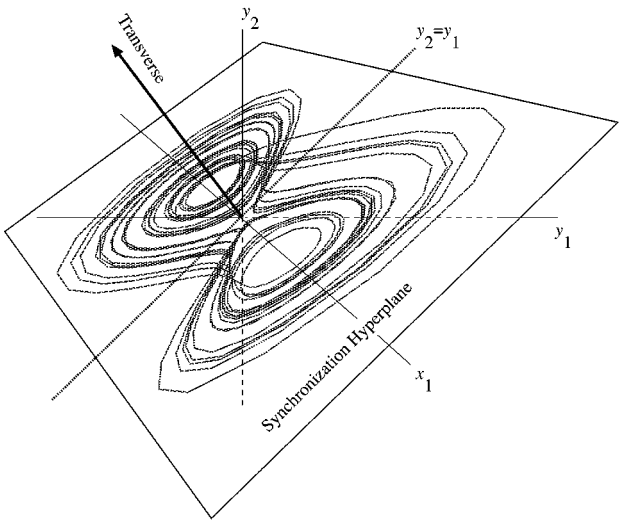

FIG. 2. A projection of the hyperplane on which the motion of the drive–response Lorenz systems takes place.

really one and the same, as we show in the next section. From here on we refer to this hyperplane as the *synchronization manifold*.

B. Some generalizations and identical synchronization

We can make several generalizations about the synchronization manifold. There is identical synchronization in any system, chaotic or not, if the motion is continually confined to a hyperplane in phase space. To see this, note that we can change coordinates with a constant linear transformation and keep the same geometry. These transformations just represent changes of variables in the equations of motion. We can assume that the hyperplane contains the origin of the coordinates since this is just a simple translation that also maintains the geometry. The result of these observations is that the space orthogonal to the synchronization manifold, which we will call the *transverse* space, has coordinates that will be zero when the motion is on the synchronization manifold. Simple rotations between pairs of synchronization manifold coordinates and transverse manifold coordinates will then suffice to give us sets of paired coordinates that are equal when the motion is on the synchronization manifold, as in the examples above.

There is another other general property that we will note, since it can eliminate some confusion. The property of having a synchronization manifold is independent of whether the system is attracted to that manifold when started away from it. The latter property is related to stability, and we take that up below. The only thing we require now is that the synchronization manifold is invariant. That is, the dynamics of the system will keep us on the manifold if we start on the manifold. Whether the invariant manifold is stable is a separate question.

For a slightly different, but equivalent, approach one should examine the paper by Tresser *et al.*[11] which approaches the formulation of identical synchronization using Cartesian products. Most of the geometric statements made here can be couched in their formulation. They also consider a more general type of chaotic driving in that formulation, which is similar to some variations we have examined.[9,12,13] In this more general case a chaotic signal is used to drive another, nonidentical system. Tresser *et al.* point out the consequences for that scheme when the driving is stable. This is also similar to what is now being called ''generalized synchronization'' (see below). We will comment more on this below.

III. DYNAMICS: SYNCHRONIZATION STABILITY

A. Stability and the transverse manifold

1. Stability for one-way coupling or driving

In our complete replacement (CR) example of two synchronized Lorenz systems, we noted that the differences $|y_1-y_2|\to 0$ and $|z_1-z_2|\to 0$ in the limit of $t\to\infty$, where t is time. This occurs because the synchronization manifold is stable. To see this let us transform to a new set of coordinates: x_1 stays the same and we let $y_\perp=y_1-y_2$, $y_\parallel=y_1+y_2$, and $z_\perp=z_1-z_2$, $z_\parallel=z_1+z_2$. What we have done here is to transform to a new set of coordinates in which three coordinates are on the synchronization manifold $(x_1,y_\parallel,z_\parallel)$ and two are on the transverse manifold ($y_\perp$ and $z_\perp$).

We see that, at the very least, we need to have $y_\perp$ and $z_\perp$ go to zero as $t\to\infty$. Thus, the zero point (0,0) in the transverse manifold must be a fixed point within that manifold. This leads to requiring that the dynamical subsystems $dy_\perp/dt$ and $dz_\perp/dt$ be stable at the (0,0) point. In the limit of small perturbations ($y_\perp$ and $z_\perp$) we end up with typical *variational* equations for the response: we approximate the differences in the vector fields by the Jacobian, the matrix of partial derivatives of the right-hand side of the (y-z) response system. The approximation is just a Taylor expansion of the vector field functions. If we let $\mathbf{F}$ be the (two-dimensional) function that is the right-hand side of the response of Eq. (1), we have

$$\begin{pmatrix}\dot{y}_\perp\\ \dot{z}_\perp\end{pmatrix}=\mathbf{F}(y_1,z_1)-\mathbf{F}(y_2,z_2)$$

$$\approx D\mathbf{F}\cdot\begin{pmatrix}y_\perp\\ z_\perp\end{pmatrix}=\begin{pmatrix}-1 & -x_1\\ x_1 & -b\end{pmatrix}\cdot\begin{pmatrix}y_\perp\\ z_\perp\end{pmatrix}, \tag{2}$$

where $y_\perp$ and $z_\perp$ are considered small. Solutions of these equations will tell us about the stability—whether $y_\perp$ or $z_\perp$ grow or shrink as $t\to\infty$.

The most general and, it appears the minimal condition for stability, is to have the Lyapunov exponents associated with Eq. (2) be negative for the transverse subsystem. We easily see that this is the same as requiring the response subsystem y_2 and z_2 to have negative exponents. That is, we treat the response as a separate dynamical system driven by x_1 and we calculate the Lyapunov exponents as usual for that *subsystem* alone. These exponents will, of course, depend on x_1 and for that reason we call them *conditional Lyapunov exponents*.[9]

TABLE I. Conditional Lyapunov exponents for two drive-response systems, the Rössler ($a=0.2$, $b=0.2$, $c=9.0$) and the Lorenz84,[14] which we see cannot be synchronized by the CR technique.

System	Drive signal	Response system	Conditional Lyapunov exponents
Rössler	x	(y,z)	$(+0.2, -0.879)$
	y	(x,z)	$(-0.056, -8.81)$
	z	(x,y)	$(+0.0, -11.01)$
Lorenz84	x	(y,z)	$(+0.0622, -0.0662)$
	y	(x,z)	$(+0.893, -0.643)$
	z	(x,y)	$(+0.985, -0.716)$

The signs of the conditional Lyapunov exponents are usually not obvious from the equations of motion. If we take the same Lorenz equations and drive with the z_1 variable, giving a dynamical system made from x_1, y_1, z_1, x_2, and y_2, we will get a neutrally stable response where one of the exponents is zero. In other systems, for example, the Rössler system that is a 3-D dynamical system, in the chaotic regime driving with the x_1 will generally not give a stable (y,z) response. Of course, these results will also be parameter dependent. We show above a table of the associated exponents for various subsystems (Table I). We see that using the present approach we cannot synchronize the Lorenz84 system. We shall see that this is not the only approach. Similar tables can be made for other systems.

We can approach the synchronization of two chaotic systems from a more general viewpoint in which the above technique of CR is a special case. This is one-way, *diffusive* coupling, also called negative feedback control. Several approaches have been shown using this technique.[15–20] What we do is add a damping term to the response system that consists of a difference between the drive and response variables:

$$\frac{d\mathbf{x}_1}{dt}=\mathbf{F}(\mathbf{x}_1) \quad \frac{d\mathbf{x}_2}{dt}=\mathbf{F}(\mathbf{x}_2)+\alpha\mathbf{E}(\mathbf{x}_1-\mathbf{x}_2), \tag{3}$$

where $\mathbf{E}$ is a matrix that determines the linear combination of $\mathbf{x}$ components that will be used in the difference and α determines the strength of the coupling. For example, for two Rössler systems we might have

$$\begin{aligned} \frac{dx_1}{dt}&=-(y_1+z_1), & \frac{dx_2}{dt}&=-(y_2+z_2)+\alpha(x_1-x_2),\\ \frac{dy_1}{dt}&=x_1+ay_1, & \frac{dy_2}{dt}&=x_2+ay_2,\\ \frac{dz_1}{dt}&=b+z_1(x_1-c), & \frac{dz_2}{dt}&=b+z_2(x_2-c), \end{aligned} \tag{4}$$

where in this case we have chosen

$$\mathbf{E}=\begin{pmatrix} 1 & 0 & 0\\ 0 & 0 & 0\\ 0 & 0 & 0 \end{pmatrix}. \tag{5}$$

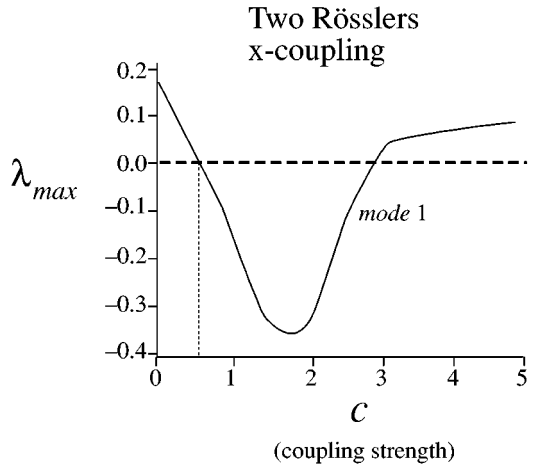

FIG. 3. The maximum transverse Lyapunov exponent $\lambda_{\max}^{\perp}$ as a function of coupling strength α in the Rössler system.

For any value of α we can calculate the Lyapunov exponents of the variational equation of Eq. (4), which is calculated similar to that of Eq. (2) except that it is three dimensional:

$$\begin{pmatrix} \frac{dx_\perp}{dt}\\ \frac{dy_\perp}{dt}\\ \frac{dz_\perp}{dt} \end{pmatrix}=\begin{pmatrix} -\alpha & -1 & -1\\ 1 & a & 0\\ z & 0 & x-c \end{pmatrix}\cdot\begin{pmatrix} x_\perp\\ y_\perp\\ z_\perp \end{pmatrix}, \tag{6}$$

where the matrix in Eq. (6) is the Jacobian of the full Rössler system plus the coupling term in the x equation. Recall Eq. (6) gives the dynamics of perturbations transverse to the synchronization manifold. We can use this to calculate the transverse Lyapunov exponents, which will tell us if these perturbations will damp out or not and hence whether the synchronization state is stable or not. We really only need to calculate the largest transverse exponent, since if this is negative it will guarantee the stability of the synchronized state. We call this exponent $\lambda_{\max}^{\perp}$ and it is a function of α. In Fig. 3 we see the dependence of $\lambda_{\max}^{\perp}$ on α. The effect of adding coupling at first is to make $\lambda_{\max}^{\perp}$ decrease. This is common and was shown to occur in most coupling situations for chaotic systems in Ref. 10. Thus, at some intermediate value of α, we will get the two Rössler systems to synchronize. However, at large α values we see that $\lambda_{\max}^{\perp}$ becomes positive and the synchronous state is no longer stable. This *desynchronization* was noted in Refs. 10, 21, and 22. At extremely large α we will slave x_2 to x_1. This is like replacing all occurrences of x_2 in the response with x_1, i.e. as $\alpha\to\infty$ we asymptotically approach the CR method of synchronization first shown above for the Lorenz systems. Hence, diffusive, one-way coupling and CR are related[16] and the asymptotic value of $\lambda_{\max}^{\perp}(\alpha\to\infty)$ tells us whether the CR method will work. Conversely, the asymptotic value of $\lambda_{\max}^{\perp}$ is determined by the stability of the subsystem that remains *uncoupled* from the drive, as we derived from the CR method.

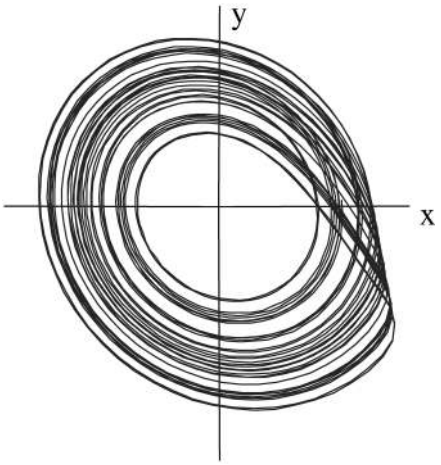

FIG. 4. Attractor for the circuit-Rössler system.

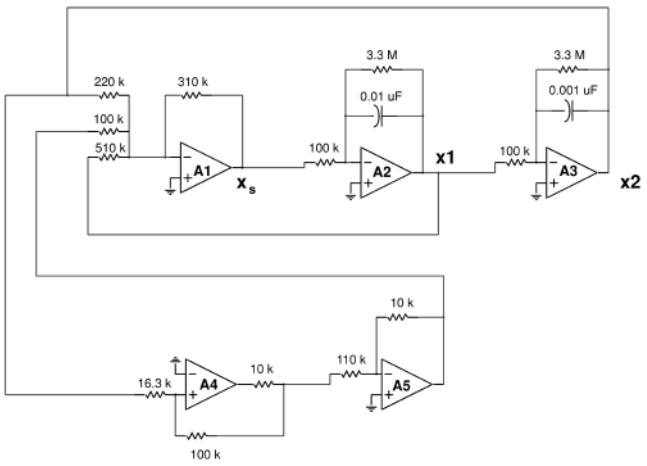

FIG. 5. Chaotic drive and response circuits for a simple chaotic system described by Eqs. (9).

2. Stability for two-way or mutual coupling

Most of the analysis for one-way coupling will carry through for mutual coupling, but there are some differences. First, since the coupling is not one way the Lyapunov exponents of one of the subsystems will not be the same as the exponents for the transverse manifold, as is the case for drive–response coupling. Thus, to be sure we are looking at the right exponents we should always transform to coordinates in which the transverse manifold has its own equations of motion. Then we can investigate these for stability:

$$\begin{aligned} \frac{dx_1}{dt} &= -(y_1+z_1)+\alpha(x_2-x_1), & \frac{dx_2}{dt} &= -(y_2+z_2) \\ & & & \quad +\alpha(x_1-x_2), \\ \frac{dy_1}{dt} &= x_1+ay_1, & \frac{dy_2}{dt} &= x_2+ay_2, \qquad (7) \\ \frac{dz_1}{dt} &= b+z_1(x_1-c), & \frac{dz_2}{dt} &= b+z_2(x_2-c). \end{aligned}$$

For coupled Rössler systems like Eq. (7) we can perform the same transformation as before. Let $x_\perp = x_1 - x_2$, $x_\parallel = x_1 + x_2$ and with similar definitions for y and z. Then examine the equations for $x_\perp$, $y_\perp$, and $z_\perp$ in the limit where these variables are very small. This leads to a variational equation as before, but one that now includes the coupling a little differently:

$$\begin{pmatrix} \frac{dx_\perp}{dt} \\ \frac{dy_\perp}{dt} \\ \frac{dz_\perp}{dt} \end{pmatrix} = \begin{pmatrix} -2\alpha & -1 & -1 \\ 1 & a & 0 \\ z & 0 & x-c \end{pmatrix} \cdot \begin{pmatrix} x_\perp \\ y_\perp \\ z_\perp \end{pmatrix}. \qquad (8)$$

Note that the coupling now has a factor of 2. However, this is the only difference. Solving Eq. (6) for Lyapunov exponents for various α values will also give us solutions to Eq. (8) for coupling values that are doubled. This use of variational equations in which we scale the coupling strength to cover other coupling schemes is much more general than might be expected. We show how it can become a powerful tool later in this paper.

The interesting thing that has emerged in the last several years of research is that the two methods we have shown so far for linking chaotic systems to obtain synchronous behavior are far from the only approaches. In the next section we show how one can design several versions of synchronized, chaotic systems.

IV. SYNCHRONIZING CHAOTIC SYSTEMS, VARIATIONS ON THEMES

A. Simple synchronization circuit

If one drives only a single circuit subsystem to obtain synchronization, as in Fig. 1, then the response system may be completely linear. Linear circuits have been well studied and are easy to match. Figure 5 is a schematic for a simple chaotic driving circuit driving a single linear subsystem.[23] This circuit is similar to the circuit that we first used to demonstrate synchronization[5] and is based on circuits developed by Newcomb.[24] The circuit may be modeled by the equations

$$\begin{aligned} \frac{dx_1}{dt} &= \alpha[-1.35x_1+3.54x_2+7.8g(x_2)+0.77x_1], \\ \frac{dx_2}{dt} &= \beta[2x_1+1.35x_2]. \end{aligned} \qquad (9)$$

The function $g(x_2)$ is a square hysteresis loop that switches from -3.0 to 3.0 at $x_2 = -2.0$ and switches back at $x_2 = 2.0$. The time factors are $\alpha = 10^3$ and $\beta = 10^2$. Equation (9) has two x_1 terms because the second x_1 term is an adjustable damping factor. This factor is used to compensate for the fact that the actual hysteresis function is not a square loop as in the g function.

The circuit acts as an unstable oscillator coupled to a hysteretic switching circuit. The amplitudes of x_1 and x_2 will

increase until x_2 becomes large enough to cause the hysteretic circuit to switch. After the switching, the increasing oscillation of x_1 and x_2 begins again from a new center.

The response circuit in Fig. 5 consists of the x_2 subsystem along with the hysteretic circuit. The x_1 signal from the drive circuit is used as a driving signal. The signals x_2' and x_1' are seen to synchronize with x_2 and x_s. In the synchronization, some glitches are seen because the hysteretic circuits in the drive and response do not match exactly. Sudden switching elements, such as those used in this circuit, are not easy to match. The matching of all elements is an important consideration in designing synchronizing circuits, although matching of nonlinear elements often presents the most difficult problem.

B. Cascaded drive-response synchronization

Once one views the creation of synchronous, chaotic systems as simply ''linking'' various systems together, a ''building block'' approach can be taken to producing other types of synchronous systems. We can quickly build on our original CR scheme and produce an interesting variation that we call a *cascaded* drive-response system (see Fig. 8). Now, provided each response subsystem is stable (has negative conditional Lyapunov exponents), both responses will synchronize with the drive and with each other.

A potentially useful outcome is that we have reproduced the drive signal x_1 by the synchronized x_3. Of course, we have $x_1=x_3$ only if all systems have the same parameters. If we vary a parameter in the drive, the difference x_1-x_3 will become nonzero. However, if we vary the responses' parameters in the same way as the drive, we will keep the null difference. Thus, by varying the response to null the difference, we can follow the internal parameter changes in the drive. If we envision the drive as a transmitter and the response as a receiver, we have a way to communicate changes in internal parameters. We have shown how this will work in specific systems (e.g., Lorenz) and implemented parameter variation and following in a real set of synchronized, chaotic circuits.[6]

With cascaded circuits, we are able to reproduce all of the drive signals. It is important in a cascaded response circuit to reproduce all nonlinearities with sufficient accuracy, usually within a few percent, to observe synchronization. Nonlinear elements available for circuits depend on material and device properties, which vary considerably between different devices. To avoid these difficulties we have designed circuits around piecewise linear functions, generated by diodes and op amps. These nonlinear elements (originally used in analog computers[25]) are easy to reproduce. Figure 6 shows schematics for drive and response circuits similar to the Rössler system but using piecewise linear nonlinearities.[26] The drive circuit may be described by

$$\frac{dx}{dt}=-\alpha(\Gamma x+\beta y+\lambda z),$$

$$\frac{dy}{dt}=-\alpha(x-\gamma y+0.02y),$$

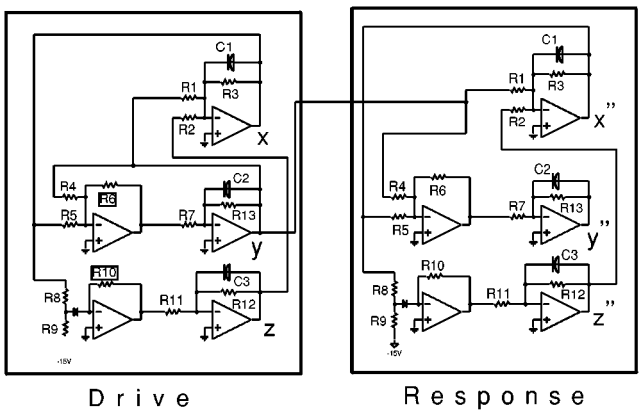

FIG. 6. Piecewise linear Rössler circuits arranged for cascaded synchronization. R1=100 kΩ, R2=200 kΩ, R3=R13=2 MΩ, R4=75 kΩ, R5=10 kΩ, R6=10 kΩ, R7=100 kΩ, R8=10 kΩ, R9=68 kΩ, R10=150 kΩ, R11=100 kΩ, R12=100 kΩ, C1=C2=C3=0.001 μF, and the diode is a type MV2101.

$$\frac{dz}{dt}=-\alpha[-g(x)-z],$$

$$g(x)=\begin{cases}0, & x\leqslant 3,\\ \mu x, & x>3,\end{cases} \tag{10}$$

where the time factor α is 10^4 s^{-1}, γ is 0.05, β is 0.5, λ is 1.0, λ is 0.133, $\Gamma=0.05$, and μ is 15. In the response system the y signal drives the (x,z) subsystem, after which the y subsystem is driven by x and y to produce y'. The extra factor of $0.02y$ in the second of Eq. (10) becomes $0.02y''$ in the response circuit in order to stabilize the op amp integrator.

C. Cuomo–Oppenheim communications scheme

A different form of cascading synchronization was applied to a simple communications scheme early on by Cuomo and Oppenheim.[27,28] They built a circuit version of the Lorenz equations using analog multiplier chips. Their setup is shown schematically in Fig. 7. They transmitted the x signal from their drive circuit and added a small speech signal. The speech signal was hidden under the broadband Lorenz signal in a process known as signal masking. At their receiver, the difference $x-x'$ was taken and found to be

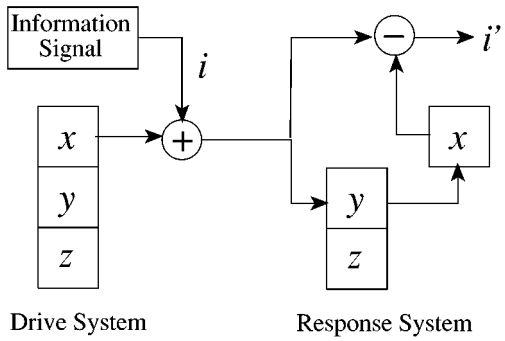

FIG. 7. Schematic for the Cuomo–Oppenheim scheme.

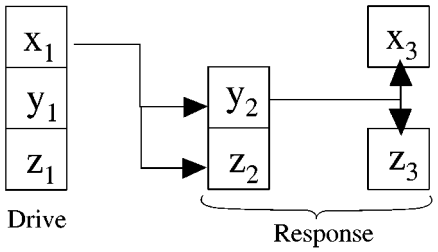

FIG. 8. Cascading scheme for obtaining synchronous chaos using complete replacement.

approximately equal to the masked speech signal (as long as the speech signal was small). Other groups later demonstrated other simple communications schemes.[29–32] It has been shown that the simple chaotic communication schemes are not ''secure'' in a technical sense.[33,34] Other encoding schemes using chaos may be harder to break, although one must consider that this description usually works by finding patterns, and chaotic systems, because they are deterministic, are often pattern generators. Later we show how one might avoid patterns in chaotic systems.

D. Nonautonomous synchronization

Nonautonomous synchronization has been accomplished in several nonautonomous systems and circuits,[35–39] but the more difficult problem of synchronizing two nonautonomous systems with separate, but identical, forcing functions has not been treated, except for the work by Carroll and Pecora.[7] In this system we start out with a cascaded version of a three-variable, nonautonomous system so as to reproduce the incoming driving signal when the systems are in synchronization (see Fig. 9). Similar to the cascaded, parameter variation scheme when the phases of the limit-cycle forcing functions are not the same, we will see a deviation from the null

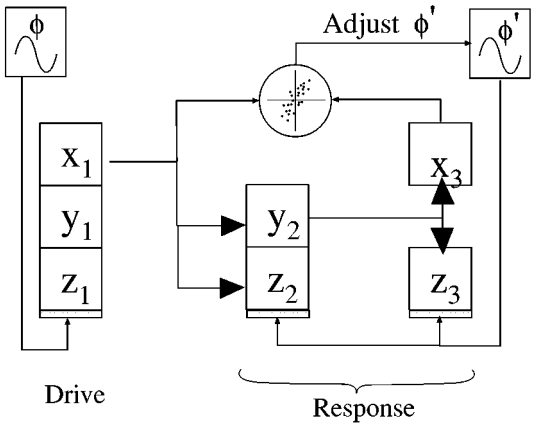

FIG. 9. Nonautonomous synchronization schematic. The local periodic drive is indicated as going into the ''bottom'' of the drive or response, but it can show up in any or all blocks. The incoming signal x_1 is compared to the outgoing x_3 using a strobe. When the periodic drives are out of phase (i.e., $\phi \neq \phi'$) we will see a pattern in the strobe x_1-x_3 diagram that will allow us to adjust ϕ' to match ϕ.

in the difference $x_1 - x_3$. We can use this deviation to adaptively correct the phase of the response forcing to bring it into agreement with the drive.[7]

A good way to do this is to use a Poincaré section consisting of x_1 and x_3, which is ''strobed'' by the response forcing cycle. If the drive and response are in sync, the section will center around a fixed point. If the phase is shifted with respect to the drive, the points will cluster in the first or third quadrants depending on whether the response phase lags or leads the drive phase, respectively. The shift in Poincaré points will be roughly linear and, hence, we know the magnitude and the sign of the phase correction. This has been done in a real circuit. See Ref. 7 for details.

E. Partial replacement

In the drive-response scenario thus far we have replaced one of the dynamical variables in the response completely with its counterpart from the drive (CR drive response). We can also do this in a partial manner as shown by Ref. 40. In the partial substitution approach we replace a response variable with the drive counterpart only in certain locations. The choice of locations will depend on which will cause stable synchronization and which are accessible in the actual physical device we are interested in building.

An example of replacement is the following system based on the Lorenz system:

$$\dot{x}_1 = \sigma(y_1 - x_1), \quad \dot{y}_1 = r x_1 - y_1 - x_1 z_1, \quad \dot{z}_1 = x_1 y_1 - b z_1,$$
$$\dot{x}_2 = \sigma(\underline{y_1} - x_2), \quad \dot{y}_2 = r x_2 - y_2 - x_2 z_2, \quad \dot{z}_2 = x_2 y_2 - b z_2. \tag{11}$$

Note the underlined driving term y_1 in the second system. The procedure here is to replace only y_2 in this equation and not in the other response equations. This leads to a variational Jacobian for the stability, which is now 3×3, but with a zero where y_1 is in the $\dot{x}_2$ equation. In general, the stability is different than CR drive response. There may be times when this is beneficial. The actual stability (variational) equation is

$$\frac{d}{dt}\begin{pmatrix} x_\perp \\ y_\perp \\ z_\perp \end{pmatrix} = D\mathbf{F}\cdot\begin{pmatrix} x_\perp \\ y_\perp \\ z_\perp \end{pmatrix} = \begin{pmatrix} -\sigma & \underline{0} & 0 \\ r - z_2 & -1 & x_2 \\ y_2 & x_2 & -b \end{pmatrix}\cdot\begin{pmatrix} x_\perp \\ y_\perp \\ z_\perp \end{pmatrix}, \tag{12}$$

where following Ref. 40 we have marked the Jacobian component that is now zero with an underline.

F. Occasional driving

Another approach is to send a drive signal only occasionally to the response and at those times we update the response variables. In between the updates we let both drive and response evolve independently. This approach was first suggested by Amritkar *et al.*[41] They discovered that this approach affected the stability of the synchronized state, in some cases causing synchronization where continuous driving would not.

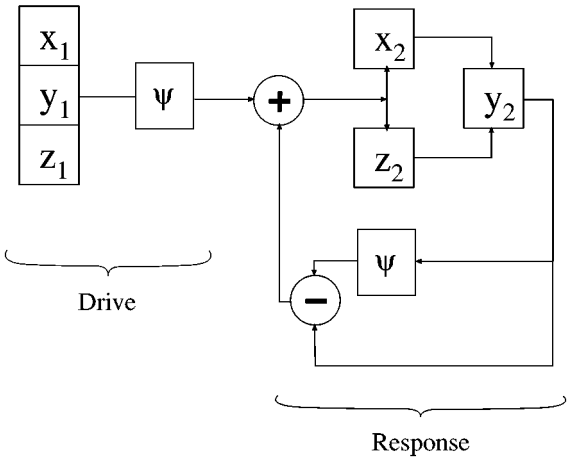

FIG. 10. Schematic for synchronous substitution using a filter.

Later this idea was applied with a view toward communications by Stojanovski *et al.*[42,43] For private communications, in principle, occasional driving should be more difficult to decrypt or break since there is less information transmitted per unit time.

G. Synchronous substitution

We are often in a position of wanting several or all drive variables at the response when we can only send one signal. For example, we might want to generate a function of several drive variables at the response, but we only have one signal coming from the drive. We show that we can sometimes substitute a response variable for its drive counterpart to serve our purpose. This will work when the response is synchronized to the drive (then the two variables are equal) and the synchronization is stable (the two variables stay equal). We refer to this practice as *synchronous substitution*. For example, this approach allows us to send a signal to the response that is a function of the drive variables and use the inverse of that function at the response to generate variables to use in driving the response. This will generally change the stability of the response.

The first application of this approach was given in Refs. 44 and 45. Other variations have also been offered, including use of an active/passive decomposition.[46]

In the original case,[44,45] strong spectral peaks in the drive were removed by a filter system at the drive and then the filtered signal was sent to the response. At the response a similar filtering system was used to generate spectral peaks from the response signals similar to those removed at the drive. These were added to the drive signal and the sum was used to drive the response as though it were the original drive variable. Schematically, this is shown in Fig. 10. In equation form we have

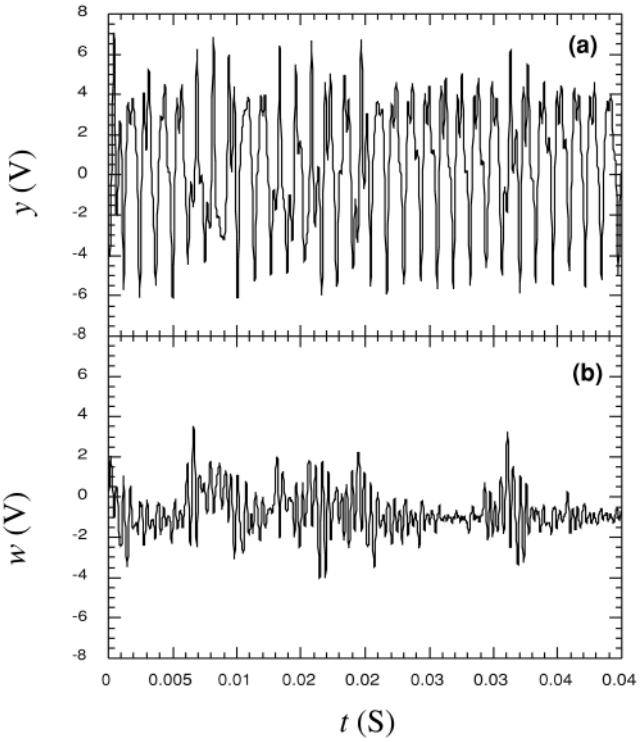

FIG. 11. The original y signal and its filtered, transmitted version w.

$$
\begin{aligned}
&\frac{dx_1}{dt}=f(x_1,y_1,z_1), \quad && \frac{dx_2}{dt}=f(x_2,u,z_2),\\
&\frac{dy_1}{dt}=g(x_1,y_1,z_1), && \frac{dy_2}{dt}=g(x_2,y_2,z_2),\\
&\frac{dz_1}{dt}=h(x_1,y_1,z_1), && \frac{dz_2}{dt}=h(x_2,u,z_2),\\
&w_1=\psi(y_1), && u=y_2-\psi(y_2)+w_1,
\end{aligned}
\tag{13}
$$

where subscripts label drive and response and ψ is a filter that passes all signals except particular, unwanted spectral peaks that it attenuates (e.g., a comb filter). At the response side we have a cascaded a system in which we use the local (response) y_2 variable to regenerate the spectral peaks by subtracting the filtered y_2 from y_2 itself and adding in the remaining signal w that was sent from the drive. If all the systems are in sync, u will equal y_1 in the drive. The test will be the following: is this system stable? In Refs. 44 and 45, Carroll showed that there do exist filters and chaotic systems for which this setup is stable. Figure 11 shows y_1 and the broadcast w signal. Hence, we can modify the drive signal and use synchronous substitution on the response end to undo the modification, all in a stable fashion. This allows us more flexibility in what types of signals we can transmit to the response.

In Ref. 47 we showed that one could use nonlinear functions to produce a drive signal. This approach also changes the stability of the response since we have a different functional relation to the drive system. An example of this is a Rössler-like circuit system using partial replacement in Ref. 47:

$$\frac{dx_1}{dt}=-\alpha(rx_1+\beta y_1+z_1), \qquad \frac{dx_2}{dt}=-\alpha(rx_2+\beta y_2+z_2),$$
$$\frac{dy_1}{dt}=-\alpha(\gamma y_1-x_1-ay_1), \qquad \frac{dy_2}{dt}=-\alpha(\gamma y_2-x_2-a\tilde{y}),$$
$$\frac{dz_1}{dt}=-\alpha[z_1-g(x_1)], \qquad \frac{dz_2}{dt}=-\alpha[z_2-g(x_2)], \tag{14}$$
$$g(x_1)=\begin{cases} 0, & \text{if } x<3 \\ 15(x_1-3), & \text{if } x\geqslant 3 \end{cases} \quad g(x_2)=\text{same form as drive } g,$$
$$\tilde{y}=-w(x_2+4.2),$$
$$w=\frac{-y_1}{x_1+4.2}.$$

What we have done above is to take the usual situation of partial replacement of y_2 with y_1 and instead transform the drive variables using the function w and send that signal to the response. Then we invert w at the response to give us a good approximation to $y_1 \approx \tilde{y}$ and drive the response using partial replacement with $\tilde{y}$. This, of course, changes the stability. The Jacobian for the response becomes

$$-\alpha\begin{pmatrix} r & \beta & 1 \\ -1+aw & \gamma & 0 \\ -g & 0 & 1 \end{pmatrix}. \tag{15}$$

With direct partial replacement (i.e., sending y_1 and using it in place of $\tilde{y}$ above) the Jacobian would not have the $+aw$ term in the first column. The circuit we built using this technique was stable.

We can write a general formulation of the synchronous substitution technique as used above.[47] We start with an n-dimensional dynamical system $d\mathbf{r}/dt=\mathbf{F}(\mathbf{r})$, where $\mathbf{r}=(x,y,z,\ldots)$. We use a general function T from $\mathbb{R}^n \to \mathbb{R}$. We send the scalar signal $w=T(x_1,y_1,z_1\ldots)$. At the response we invert T to give an approximation to the drive variable x_1, namely $\tilde{x}=T_1(w,y_2,z_2,\ldots)$, where T_1 is the inverse of T in the first argument. By the implicit function theorem T_1 will exist if $\partial T/\partial x \neq 0$. Synchronous substitution comes in T_1 where we normally would need $y_1,z_1,\ldots$, to invert T. Since we do not have access to those variables, we use their synchronous counterparts $y_2,z_2,\ldots$, in the response.

Using this formulation in the case of partial replacement or complete replacement of x_2 or some other functional dependence on w in the response we now have a new Jacobian in our variational equation:

$$\frac{d\,\delta\mathbf{r}}{dt}=[D_{\mathbf{r}}\mathbf{F}+D_w\mathbf{F}\ D_{\mathbf{r}}T_1]\cdot\delta\mathbf{r}, \tag{16}$$

where we have assumed that the response vector field $\mathbf{F}$ has an extra argument, w, to account for the synchronous substitution. In Eq. (16) the first term is the usual Jacobian and the second term comes from the dependence on w. Note that, if we use complete replacement of x_2 with x_1, the $D_x\mathbf{F}$ part of the first term in Eq. (16) would be zero.

There are other variations on the theme of synchronous substitution. We introduce another here since it leads to a special case that is used in control theory and that we have recently exploited. One way to guarantee synchronization would be to transmit all drive variables and couple them to the response using negative feedback, viz.

$$d\mathbf{x}^{(2)}/dt=\mathbf{F}(\mathbf{x}^{(2)})+c(\mathbf{x}^{(1)}-\mathbf{x}^{(2)}), \tag{17}$$

where, unlike before, we now use superscripts in parentheses to refer to the drive (1) and the response (2) variables and $\mathbf{x}^{(1)}=(x_1^{(1)},x_2^{(1)},\ldots,x_n^{(1)})$, etc. With the right choice of coupling strength c, we could always synchronize the response. But again we are limited in sending only one signal to the response. We do the following, which makes use of synchronous substitution.

Let $S:\mathbb{R}^n \to \mathbb{R}^n$ be a differentiable, invertible transformation. We construct $\mathbf{w}=S(\mathbf{x}^{(1)})$ at the drive and transmit the first component w_1 to the response. At the response we generate the vector $\mathbf{u}=S(\mathbf{x}^{(2)})$. Near the synchronous state $\mathbf{u} \approx \mathbf{w}$. Thus we have approximations at the response to the components w_i that we do not have access to. We therefore attempt to use Eq. (17) by forming the following:

$$\frac{d\mathbf{x}^{(2)}}{dt}=\mathbf{F}(\mathbf{x}^{(2)})+c[S^{-1}(\tilde{\mathbf{w}})-\mathbf{x}^{(2)}], \tag{18}$$

where in order to approximate $c(\mathbf{x}^{(1)}-\mathbf{x}^{(2)})$ we have used synchronous substitution to form $\tilde{\mathbf{w}}(w_1,u_2,u_3,\ldots,u_n)$ and applied the inverse transformation S^{-1}.

All the rearrangements using synchronous substitution and transformations may seem like a lot of pointless algebra, but the use of such approaches allows one to transmit one signal and synchronize a response that might not be synchronizable otherwise as well as to guide in the design of synchronous systems. Moreover, a particular form of the S transformation leads us to a commonly used control-theory

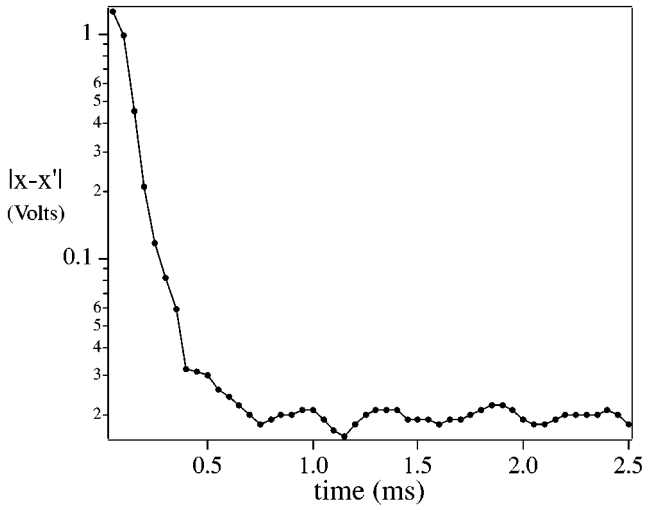

FIG. 12. The BK method is demonstrated on the piecewise-linear Rössler circuit. The difference in the X variables of receiver and transmitter is shown to converge to about 20 mV in under one cycle of the period-1 orbit (about 1 ms). The plot is an average of 100 trials.

method. The synchronous substitution formalism allows us to understand the origin of the control-theory approach. We show this in the next section.

H. Control theory approaches, a special case of synchronous substitution

Suppose in our above use of synchronous substitution the transformation S is a linear transformation. Then $S^{-1}(\tilde{\mathbf{w}})-S^{-1}(\mathbf{u})=S^{-1}(\tilde{\mathbf{w}}-\mathbf{u})$, and since $\tilde{\mathbf{w}}-\mathbf{u}$ has only its first component as nonzero, we can write $\tilde{\mathbf{w}}-\mathbf{u}=[\mathbf{K}^T(\mathbf{x}^{(1)}-\mathbf{x}^{(2)}),0,0,...,0]$, where $\mathbf{K}^T$ is the first row of S. Then the coupling term $cS^{-1}(\tilde{\mathbf{w}}-\mathbf{u})$ becomes $\mathbf{B}\mathbf{K}^T(\mathbf{x}^{(1)}-\mathbf{x}^{(2)})$, where $\mathbf{B}$ is the first column of S^{-1} and we have absorbed the coupling constant c into $\mathbf{B}$. This form of the coupling (called BK coupling from here on) is common in control theory.[48] We can see where it comes from. It is an attempt to use a linear coordinate transformation (S) to stabilize the synchronous state. Because we can only transmit one signal (one coordinate) we are left with a simpler form of the coupling that results from using response variables (synchronous substitution) in place of the missing drive variables.

Recently, experts in control theory have begun to apply BK and other control-theory concepts to the task of synchronizing chaotic systems. We will not go into all the details here, but good overviews and explanations on the stability of such approaches can be found in Refs. 49–52. In the following sections we show several explicit examples of using the BK approach in synchronization.

I. Optimization of BK coupling

Our own investigation of the BK method began with applying it to the piecewise-linear Rossler circuits. As is usually pointed out (e.g., see Peng *et al.*[53]), the problem is reduced to finding an appropriate BK combination resulting in negative Lyapunov exponents at the receiver. The piecewise-linear Rossler systems (see above) lend themselves well to this task as the stability is governed by two constant Jacobian matrices, and the Lyapunov exponents are readily determined. To seek out the proper combinations of $\mathbf{B}$'s and $\mathbf{K}$'s, we employ an optimization routine in the six-dimensional space spanned by the coupling parameters. From a six-dimensional grid of starting points in BK space, we seek out local minima of the largest real part of the eigenvalue of the response Jacobian $[\mathbf{J}-\mathbf{B}\mathbf{K}^T]$.

By limiting the size of the coupling parameters and collecting all of the deeply negative minima, we find that we can choose from a number of BK sets that ensure fast and robust synchronization. For example, the minimization routine reveals, among others, the following pair of minima well separated in BK space: $\mathbf{B}_1=\{-2.04,0.08,0.06\}$ $\mathbf{K}1=\{-1.79,-2.17,-1.84\}$, and $\mathbf{B}_2=\{0.460,2.41,0.156\}$ $\mathbf{K}_2=\{-1.37,1.60,2.33\}$. The real parts of the eigenvalues for these sets are -1.4 and -1.3, respectively. In Fig. 12, we show the fast synchronization using $\mathbf{B}_1\mathbf{K}_1{}^T$ as averaged over 100 runs, switching on the coupling at $t=0$. The time of the period-1 orbit in the circuit is about 1 ms, in which time the synchronization error is drastically reduced by about two orders of magnitude.

Similarly, we can apply the method to the volume preserving hyperchaotic map system of section x. The only difference is that we now wish to minimize the largest norm of the eigenvalues of the response Jacobian. With our optimization routine, we are able to locate eigenvalues on the order of 10^{-4}, corresponding to Lyapunov exponents around -9.

J. Hyperchaos synchronization

Most of the drive–response synchronous, chaotic systems studied so far have had only one positive Lyapunov exponent. More recent work has shown that systems with more than one positive Lyapunov exponent (called hyperchaotic systems) can be synchronized using one drive signal. Here we display several other approaches.

A simple way to construct a hyperchaotic system is to use two, regular chaotic systems. They need not be coupled; just the amalgam of both is hyperchaotic. Tsimiring and Suschik[54] recently made such a system and considered how one might synchronize a duplicate response. Their approach has elements similar to the use of synchronous substitution we mentioned above. They transmit a signal, which is the sum of the two drive systems. This sum is coupled to a sum of the same variables from the response. When the systems are in sync the coupling vanishes and the motion takes place on an invariant hyperplane and hence is identical synchronization.

An example of this situation using one-dimensional systems is the following:[54]

$$
\begin{aligned}
&x_1(n+1)=f_1[x_1(n)], \quad x_2(n+1)=f_2[x_2(n)],\\
&w=f_1[x_1(n)]+f_2[x_2(n)]-f_1[y_1(n)]-f_2[y_2(n)]\\
&\quad=\text{transmitted signal},\\
&y_1(n+1)=f_1[y_1(n)]+\epsilon\{f_1[x_1(n)]+f_2[x_2(n)]\\
&\qquad -f_1[y_1(n)]-f_2[y_2(n)]\},\\
&y_2(n+1)=f_2[y_2(n)]+\epsilon\{f_1[x_1(n)]+f_2[x_2(n)]\\
&\qquad -f_1[y_1(n)]-f_2[y_2(n)]\},
\end{aligned}
\tag{19}
$$

Linear stability analysis, as we introduced above, shows that the synchronization manifold is stable.[54] Tsimring and Suschik investigated several one-dimensional maps (tent, shift, logistic) and found that there were large ranges of coupling ϵ, where the synchronization manifold was stable. For certain cases they even got analytic formulas for the Lyapunov multipliers. However, they did find that noise in the communications channel, represented by noise added to the transmitted signal w, did degrade the synchronization severely, causing bursting. The same features showed up in their study of a set of drive-response ODEs (based on a model of an electronic synchronizing circuit). The reasons for the loss of synchronization and bursting are the same as in our study of the coupled oscillators below. There are local instabilities that cause the systems to diverge momentarily, even above Lyapunov synchronization thresholds. Any slight noise tends to keep the systems apart and ready to diverge when the trajectories visit the unstable portions of the attractors. Whether this can be ''fixed'' in practical devices so that multiplexing can be used is not clear. Our study below of synchronization thresholds for coupled systems suggests that for certain systems and coupling schemes we can avoid bursting, but more study of this phenomenon for hyperchaotic/multiplexed systems has to be done. Perhaps a BK approach may be better at eliminating bursts since it can be optimized. This remains to be seen.

The issue of synchronizing hyperchaotic systems was addressed by Peng *et al.*[53] They started with two identical hyperchaotic systems, $\dot{\mathbf{x}}=\mathbf{F}(\mathbf{x})$ and $\dot{\mathbf{y}}=\mathbf{F}(\mathbf{y})$. Their approach was to use the BK method to synchronize the systems. As before, the transmitted signal was $w=\mathbf{K}^T\mathbf{x}$ and we add a coupling term to the $\mathbf{y}$ equations of motion: $\dot{\mathbf{y}}=\mathbf{F}(\mathbf{y})+\mathbf{B}(w-v)$, where $\mathbf{v}=\mathbf{K}^T\mathbf{y}$. Peng *et al.* show that for many cases one can choose $\mathbf{K}$ and $\mathbf{B}$ so that the $\mathbf{y}$ system synchronizes with the $\mathbf{x}$ system. This and the work by Tsimring and Suschik solve a long-standing question about the relation between the number of drive signals that need to be sent to synchronize a response and the number of positive Lypunov exponents, namely that there is no relation, in principle. Many systems with a large number of positive exponents can still be synchronized with one drive signal. Practical limitations will surely exist, however. The latter still need to be explored.

Finally, we mention that synchronization of hyperchaotic systems has been achieved in experiments. Tamasevicius *et al.*[25] have shown that such synchronization can be accomplished in a circuit. They built circuits that consisted of either mutually coupled or unidirectionally coupled 4-D oscillators. They show that for either coupling both positive conditional Lypunov exponents of the ''uncoupled'' subsystems become negative as the coupling is increased. They go on to further show that they must be above a critical value of coupling which is found by observing the absence of a blowout bifurcation.[55–57] Such a demonstration in a circuit is important, since this proves at once that hyperchaos synchronization has some robustness in the presence of noise and parameter mismatch.

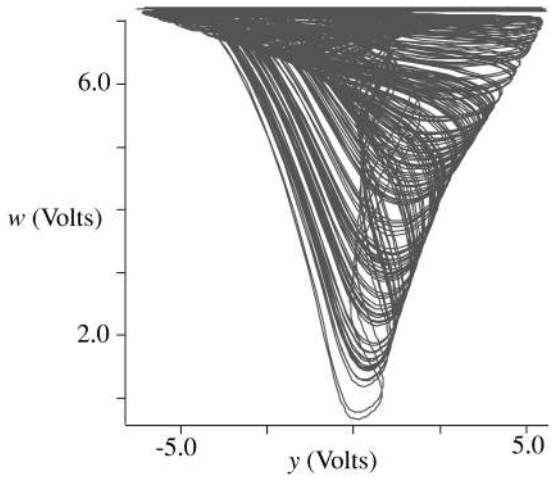

FIG. 13. A projection of the dynamics of the hyperchaotic circuit based on the 4-D Rössler equations.

We constructed a four-dimensional piecewise-linear circuit based on the hyperchaotic Rössler equations.[53,58] The modified equations are as follows:

$$
\begin{aligned}
\frac{dx}{dt}&=-0.05x-0.502y-0.62z,\\
\frac{dy}{dt}&=x+0.117y+0.402w,\\
\frac{dz}{dt}&=g(x)-1.96z,\\
\frac{dw}{dt}&=h(w)-0.148z+0.18w,
\end{aligned}
$$

where

$$
\begin{aligned}
g(x)&=10(x-0.6), && x>0.6,\\
&=0, && x<0.6,\\
h(w)&=-0.412(w-3.8), && w>3.8,\\
&=0, && w<3.8.
\end{aligned}
$$

One view of the hyperchaotic circuit is shown in the plot of w vs y in Fig. 13. Again, as with the 3-D Rossler circuit, the 4-D circuit is synchronized rapidly and robustly with the BK method. In this circuit, we are aided by the fact that the dynamics are most often driven by one particular matrix out

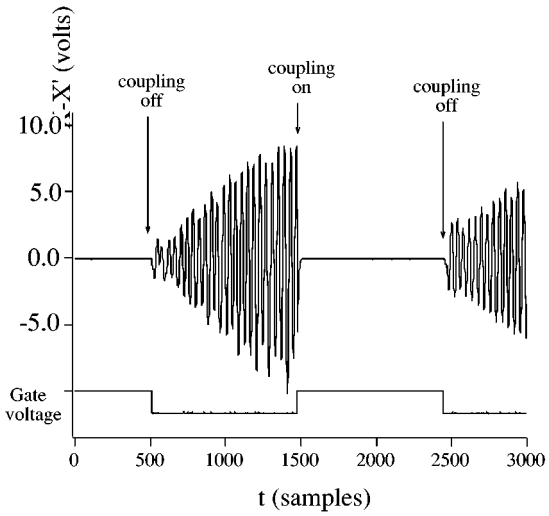

FIG. 14. The BK method as applied to the hyperchaotic circuit. The coupling is switched on when the pictured gate voltage is high, and **B** is effectively {0,0,0,0} when the gate voltage is low. The sample rate is 20 μs/sample.

of the four possible Jacobians. We have found that minimization of the real eigenvalues in the most-visited matrix is typically sufficient to provide overall stability. Undoubtedly there are cases in which this fails, but we have had a high level of success using this technique. A more detailed summary of this work will be presented elsewhere, so we briefly demonstrate the robustness of the synchronization in Fig. 14. The coupling parameters in this circuit are given by $\mathbf{B}=\{0.36,2.04,-1.96,0.0\}$ and $\mathbf{K}=\{-1.97,2.28,0,1.43\}$.

K. Synchronization as a control theory observer problem

A control theory approach to observing a system is a similar problem to synchronizing two dynamical systems. Often the underlying goal is the synchronization of the observer dynamical system with the observed system so the observed system's dynamical variables can be determined fully from knowing only a few of the observed system's variables or a few functions of those variables. Often we have only a scalar variable (or time series) from the observed system and we want to recreate all the observed system's variables.

So, Ott, and Dayawansa follow such approaches in Ref. 59. They showed that a local control theory approach based essentially on the Ott–Grebogi–Yorke technique.[60] The technique does require knowledge of the local structure of stable and unstable manifolds. In an approach that is closer to the ideas of drive-response synchronization presented above Brown *et al.*[61–64] showed that one can observe a chaotic system by synchronizing a model to a time series or scalar signal from the original system. They showed further that one could often determine a set of maps approximating the dynamics of the observed system with such an approach. Such maps could reliably calculate dynamical quantities such as Lyapunov exponents. Brown *et al.* went much further and showed that such methods could be robust to additive noise. Somewhat later, Parlitz also used these ideas to explore the determination of an observed system's parameters.[65]

L. Volume-preserving maps and communications issues

Most of the chaotic systems we describe here are based on flows. It is also useful to work with chaotic circuits based on maps. Using map circuits allows us to simulate volume-preserving systems. Since there is no attractor for a volume-preserving map, the map motion may cover a large fraction of the phase space, generating very broadband signals.

It seems counterintuitive that a nondissipative system may be made to synchronize, but in a multidimensional volume-preserving map, there must be at least one contracting direction so that volumes in phase space are conserved. We may use this one direction to generate a stable subsystem. We have used this technique to build a set of synchronous circuits based on the standard map.[66]

In hyperchaotic systems, there are more than one positive Lyapunov exponent and for a map this may mean that the number of expanding directions exceeds the number of contracting directions, so that there are no simple stable subsystems for a one-drive setup. We may, however, use the principle of synchronous substitution (described in Sec. VI below) or its specialization to the BK to generate various synchronous subsystems. We have built a circuit to simulate the following map:[67]

$$\left.\begin{aligned} x_{n+1} &= -(\tfrac{4}{3})\,x_n + z_n \\ y_{n+1} &= (\tfrac{1}{3})\,y_n + z_n \\ z_{n+1} &= x_n + y_n \end{aligned}\right\} \bmod 2, \tag{20}$$

where ''mod(2)'' means take the result modulus ± 2. This map is quite similar to the cat map[68] or the Bernoulli shift in many dimensions. The Lyapunov exponents for this map (determined from the eigenvalues of the Jacobian) are 0.683, 0.300, and -0.986.

We may create a stable subsystem of this map using the method of synchronous substitution.[47] We produce a new variable $w_n = z_n + \gamma x_n$ from the drive system variables, and reconstruct a driving signal $\tilde{z}_n$ at the response system:

$$\begin{aligned} &w_n = z_n + \gamma x_n, \quad \tilde{z}_n = w_n - \gamma x'_n, \\ &x'_{n+1} = -(\tfrac{4}{3})\,x'_n + \tilde{z}_n, \quad y'_{n+1} = (\tfrac{1}{3})\,y'_n + \tilde{z}_n, \end{aligned} \tag{21}$$

where the modulus function is assumed. In the circuit, we used $\gamma = -4/3$, although there is a range of values that will work. We were able to synchronize the circuits adequately in spite of the difficulty of matching the modulus functions.

The transmitted signal from this circuit has essentially a flat power spectrum and approximately a delta-function autocorrelation, making the signal a good alternative to a conventional pseudonoise signal. Our circuit is in essence a self-synchronizing pseudonoise generator. We present more information on this system, its properties and communications issues in Refs. 67 and 69.

M. Using functions of drive variables and information

An interesting approach involving the generation of new synchronizing vector fields was taken by Kocarev.[70,71] This is an approach similar to synchronous substitution that uses an invertible function of the drive dynamical variables and the information signal to drive the response, rather than just using one of the variables itself as in the CR approach. Then on the response the function is inverted using the fact that the system is close to synchronization.

Schematically, this looks as follows. On the drive end there is a dynamical system $\dot{\mathbf{x}}=\mathbf{F}(\mathbf{x},s)$, where s is the transmitted signal and is a function of $\mathbf{x}$ and the information $i(t)$, $s=h(\mathbf{x},i)$. On the receiver end there is an identical dynamical system set up to extract the information: $\dot{\mathbf{y}}=\mathbf{F}(\mathbf{y},s)$ and $i^R=h^{-1}(\mathbf{y},s)$. When the systems are in sync $i^R=i$. We have shown this is useful by using XOR as our h function in the volume-preserving system.[69]

N. Synchronization in other physical systems

Until now we have concentrated on circuits as the physical systems that we want to synchronize. Other work has shown that one can also synchronize other physical systems such as lasers and ferrimagnetic materials undergoing chaotic dynamics.

In Ref. 72 Roy and Thornburg showed that lasers that were behaving chaotically could be synchronized. Two solid state lasers can couple through overlapping electromagnetic lasing fields. The coupling is similar to mutual coupling shown in Sec. III A 3, except that the coupling is negative. This causes the lasers to actually be in oppositely signed states. That is, if we plot the electric field for one against the other we get a line at $-45°$ rather than the usual 45°. This is still a form of synchronization. Actually since Roy and Thornburg only examined intensities the synchronization was still of the normal, 45° type. Colet and Roy continued to pursue this phenomenon to the point of devising a communications scheme using synchronized lasers.[73] This work was recently implemented by Alsing *et al.*[74] Such laser synchronization opens the way for potential uses in fiberoptics.

Peterman *et al.*[75] showed a novel way to synchronize the chaotic, spin-wave motion in rf pumped yttrium iron garnet. In these systems there are fast and slow dynamics. The fast dynamics amounts to sinusoidal oscillations at GHz frequencies of the spin-wave amplitudes. The slow dynamics governs the amplitude envelopes of the fast dynamics. The slow dynamics can be chaotic. Peterman *et al.* ran their experiments in the chaotic regimes and recorded the slow dynamical signal. They then ''played the signals back'' at a later time to drive the system and cause it to synchronize with the recorded signals. This shows that materials with such high-frequency dynamics are amenable to synchronization schemes.

O. Generalized synchronization

In their original paper on synchronization Afraimovich *et al.* investigated the possibility of some type of synchronization when the parameters of the two coupled systems do not match. Such a situation will certainly occur in real, physical systems and is an important question. Their study showed that for certain systems, including the 2-D forced system they studied, one could show that there was a more general relation between the two coupled systems. This relationship was expressed as a one-to-one, smooth mapping between the phase space points in each subsystem. To put this more mathematically, if the full system is described by a 4-D vector (x_1,y_1,x_2,y_2), then there exists smooth, invertible function ϕ from (x_1,y_1) to (x_2,y_2).

Thus, knowing the state of one system enables one, in principle, to know the state of the other system, and vice versa. This situation is similar to identical synchronization and has been called *generalized synchronization*. Except in special cases, like that of Afraimovich *et al.*, rarely will one be able to produce formulae exhibiting the mapping ϕ. Proving generalized synchronization from time series would be a useful capability and sometimes can be done. We show how below. The interested reader should examine Refs. 76–78 for more details.

Recently, several attempts have been made to generalize the concept of general synchronization itself. These begin with the papers by Rul'kov *et al.*[76,79] and onto a paper by Kocarev and Parlitz.[80] The central idea in these papers is that for the drive-response setup, if the response is stable (all Lypunov exponents are negative), then there exists a manifold in the joint drive-response phase space such that there is a function from the drive (X) to the response (Y), $\phi:X\rightarrow Y$. In plain language, this means we can predict the response state from that of the drive (there is one point on the response for each point on the drive's attractor) and the points of the mapping ϕ lie on a smooth surface (such is the definition of a manifold).

This is an intriguing idea and it is an attempt to answer the question we posed in the beginning of this paper, namely, does stability determine geometry? These papers would answer yes, in the drive-response case the geometry is a manifold that is ''above'' the drive subspace in the whole phase space. The idea seems to have some verification in the studies we have done so far on identical synchronization and in the more particular case of Afraimovich–Verichev–Rabinovich generalized synchronization. However, there are counterexamples that show that the conclusion cannot be true.

First, we can show that there are stable drive-response systems in which the attractor for the whole system is not a smooth manifold. Consider the following system:

$$\dot{\mathbf{x}}=\mathbf{F}(\mathbf{x}) \quad \dot{z}=-\eta z+x_1, \tag{22}$$

where $\mathbf{x}$ is a chaotic system and $\eta>0$. The z system can be viewed as a filter (LTI or low-pass type) and is obviously a stable response to the drive $\mathbf{x}$. It is now known that certain filters of this type lead to an attractor in which there is a map (often called a graph) ϕ of the drive to the response, but the mapping is not smooth. It is continuous and so the relation between the drive and response is similar to that of the real

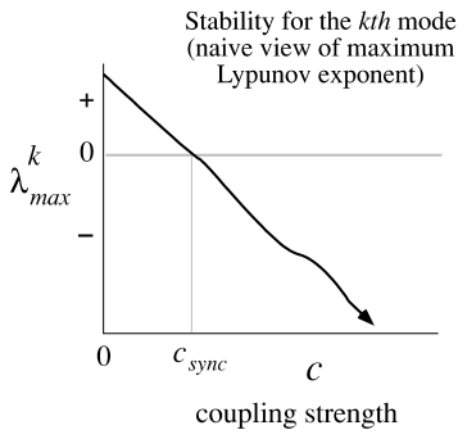

FIG. 15. A naive view of the stability of a transverse mode in an array of synchronous chaotic systems as a function of coupling c.

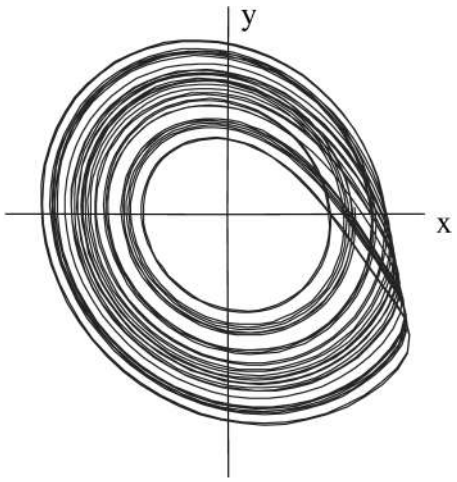

FIG. 16. The circuit Rössler attractor.

line and the Weierstrass function above it. This explains why certain filters acting on a time series can increase the dimension of the reconstructed attractor.[81,82]

We showed that certain statistics could detect this relationship,[82] and we introduce those below. Several other papers have proven the nondifferentiability property rigorously and have investigated several types of stable filters of chaotic systems.[83–89] We note that the filter is just a special case of a stable response. The criteria for smoothness in any drive-response scenario is that the least negative conditional Lypunov exponents of the response must be less than the most negative Lypunov exponents of the drive.[87,90] One can get a smooth manifold if the response is *uniformly contracting*, that is, the stability exponents are *locally* always negative.[87,91] Note that if the drive is a noninvertible dynamical system, then things are ''worse.'' The drive-response relation may not even be continuous and may be many valued, in the latter case there is not even a function ϕ from the drive to the response.

There is an even simpler counterexample that no one seems to mention that shows that stability does not guarantee that ϕ exists and this is the case of period-2 behavior (or any multiple period behavior). If the drive is a limit cycle and the response is a period doubled system (or higher multiple-period system), then for each point on the drive attractor there are two (or more) points on the response attractor. One cannot have a function under such conditions and there is no way to predict the state of the response from that of the drive. Note that there is a function from response to the drive in this case. Actually, any drive-response system that has the overall attractor on an invariant manifold that is not diffeomorphic to a hyperplane will have the same, multivalued relationship and there will be no function ϕ.

Hence, the hope that a stable response results in a nice, smooth, predictable relation between the drive and response cannot always be realized and the answer to our question of whether stability determines geometry is ''no,'' at least in the sense that it does not determine one type of geometry. Many are possible. The term general synchronization in this case may be misleading in that it implies a simpler drive-response relation than may exist. However, the stable drive–response scenario is obviously a rich one with many possible dynamics and geometries. It deserves more study.

V. COUPLED SYSTEMS: STABILITY AND BIFURCATIONS

A. Stability for coupled, chaotic systems

Let us examine the situation in which we have coupled, chaotic systems, in particular N diffusively coupled, m-dimensional chaotic systems:

$$\frac{d\mathbf{x}^{(i)}}{dt}=\mathbf{F}(\mathbf{x}^{(i)})+c\mathbf{E}(\mathbf{x}^{(i+1)}+\mathbf{x}^{(i-1)}-2\mathbf{x}^{(i)}), \tag{23}$$

where $i=1,2,...,N$ and the coupling is circular $(N+1=1)$. The matrix $\mathbf{E}$ picks out the combination of nearest neighbor coordinates that we want to use in our coupling and c determines the coupling strength. As before, we want to examine the stability of the transverse manifold when all the ''nodes'' of the system are in synchrony. This means that $\mathbf{x}^{(1)}=\mathbf{x}^{(2)}=\cdots=\mathbf{x}^{(N)}$, which defines an m-dimensional hyperplane, the synchronization manifold. We show in Ref. 10 that the way to analyze the transverse direction stability is to transform to a basis in Fourier spatial modes. We write $\mathbf{A}_k=(1/N)\Sigma_i\mathbf{x}_{(i)}e^{-2\pi ik/N}$. When N is even (which we assume for convenience), we have $N/2+1$ modes that we label with $k=0,1,...,N/2$. For $k=0$ we have the synchronous mode equation, since this is just the average of identical systems:

$$\dot{\mathbf{A}}_0=\mathbf{F}(\mathbf{A}), \tag{24}$$

which governs the motion on the synchronization manifold. For the other modes we have equations that govern the motion in the transverse directions. We are interested in the stability of these modes (near their zero value) when their amplitudes are small. This requires us to construct the variational equation with the full Jacobian analogous to Eq. (2). In the original $\mathbf{x}^{(i)}$ coordinates the Jacobian (written in block form) is

$$\begin{pmatrix} D\mathbf{F}-2c\mathbf{E} & c\mathbf{E} & 0 & \cdots & c\mathbf{E} \\ c\mathbf{E} & D\mathbf{F}-2c\mathbf{E} & c\mathbf{E} & 0 & \cdots \\ 0 & c\mathbf{E} & D\mathbf{F}-2c\mathbf{E} & c\mathbf{E} & \cdots \\ \vdots & \vdots & & & \\ c\mathbf{E} & \cdots & 0 & c\mathbf{E} & D\mathbf{F}-2c\mathbf{E} \end{pmatrix}, \tag{25}$$

where each block is $m\times m$ and is associated with a particular node $\mathbf{x}^{(i)}$. In the mode coordinates the Jacobian is block diagonal, which simplifies finding the stability conditions,

$$\begin{pmatrix} D\mathbf{F} & 0 & 0 & \cdots & c \\ 0 & D\mathbf{F}-4c\mathbf{E}\sin^2[\pi/N] & 0 & 0 & \cdots \\ \vdots & \vdots & & \vdots & \vdots \\ 0 & \cdots & 0 & D\mathbf{F}-4c\mathbf{E}\sin^2[\pi k/N] & \cdots \\ & & & \vdots & \end{pmatrix}, \tag{26}$$

where each value of $k\neq 0$ or $k\neq N/2$ occurs twice, once for the ''sine'' and once for the ''cosine'' modes. We want the transverse modes represented by sine and cosine spatial disturbances to die out, leaving only the $k=0$ mode on the synchronization manifold. At first sight what we want for stability is for all the blocks with $k\neq 0$ to have negative Lypunov exponents. We will see that things are not so simple, but let us proceed with this naive view.

Figure 15 shows the naive view of how the maximum Lypunov exponent for a particular mode block of a transverse mode might depend on coupling c. There are four features in the naive view that we will focus on.

(1) As the coupling increases from 0 we go from the Lyapunov exponents of the free oscillator to decreasing exponents until for some threshold coupling c_{sync} the mode becomes stable.
(2) Above this threshold we have stable synchronous chaos.
(3) We suspect that as we increase the coupling the exponents will continue to decrease.
(4) We can now couple together as many chaotic oscillators as we like using a coupling $c>c_{\text{sync}}$ and always have a stable synchronous state.

We already know from Fig. 3 that this view cannot be correct [increasing c may desynchronize the array—feature (3)], but we will now investigate these issues in detail. Below we will use a particular coupled, chaotic system to show that there are counterexamples to all four of these ''features.''

We first note a scaling relation for Lypunov exponents of modes with different k's. Given any Jacobian block for a mode k_1 we can always write it in terms of the block for another mode k_2, viz.,

$$D\mathbf{F}-4\mathbf{C}\sin^2[\pi k_1/N]=D\mathbf{F}-4c\mathbf{E}\left(\frac{\sin^2[\pi k_1/N}{\sin^2[\pi k_2/N]}\right)\times\sin^2[\pi k_2/N], \tag{27}$$

where we see that the effect is to shift the coupling by the factor $\sin^2(\pi k_1/N)/\sin^2(\pi k_2/N)$. Hence, given any mode's stability plot (as in Fig. 3) we can obtain the plot for any other mode by rescaling the coupling. In particular, we need only calculate the maximum Lypunov exponent for mode 1 ($\lambda^1_{\max}$) and then the exponents for all other modes $k>1$ are generated by ''squeezing'' the $\lambda^1_{\max}$ plot to smaller coupling values.

This scaling relation, first shown in Ref. 10, shows that as the mode's Lypunov exponents decrease with increasing c values the longest-wavelength mode k_1 will be the *last* to become stable. Hence, we first get the expected result that the longest wavelength (with the largest coherence length) is the least stable for small coupling.

B. Coupling thresholds for synchronized chaos and bursting

To test our four features we examine the following system of four Rossler-like oscillators diffusively coupled in a circle, which has a counterpart in a set of four circuits we built for experimental tests,[10]

$$\begin{aligned} dx/dt &= -\alpha(\Gamma x+\beta y+\lambda z), \\ dy/dt &= \alpha(x+\gamma y), \\ dz/dt &= \alpha[g(x)-z], \end{aligned} \tag{28}$$

where g is a piece-wise linear function that ''turns on'' when x crosses a threshold and causes the spiraling out behavior to ''fold'' back toward the origin,

$$g(x)=\begin{cases} 0, & x\leqslant 3, \\ \mu x', & x>3. \end{cases} \tag{29}$$

For the values $\alpha=10^4\ \text{s}^{-1}$, $\Gamma=0.05$, $\beta=0.5$, $\lambda=1.0$, $\gamma=0.133$, and $\mu=15.0$ we have a chaotic attractor very similar to the Rossler attractor (see Figs. 4 and 16).

We couple four of these circuits through the y component by adding the following term to each system's y equation: $c(y_{i+1}+y_{i-1}-2y_i)$, where the indices are all mod 4.

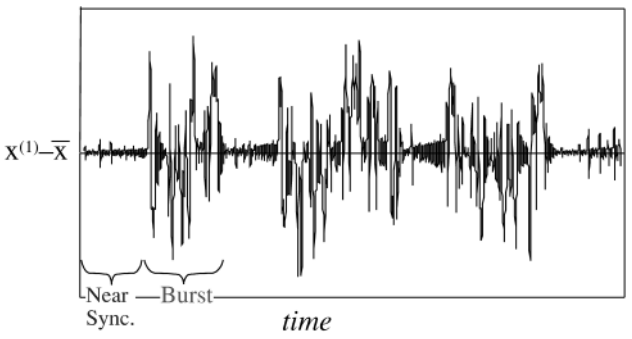

FIG. 17. The Instantaneous difference, $d=x_1-\bar{x}$, in the y-coupled circuit-Rössler system as a function of time.

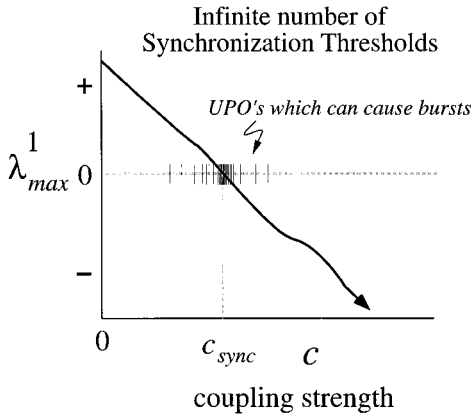

FIG. 18. The schematic plot of ''synchronization'' threshold showing thresholds for individual UPOs.

This means the coupling matrix **E** has just one nonzero element, $E_{22}=1$. A calculation of the mode Lypunov exponents indeed shows that the longest-wavelength mode becomes stable last at $c_{\text{sync}}=0.063$. However, when we examine the behavior of the so-called synchronized circuits above the threshold we see unexpected behaviors. If we take $\bar{x}$ to be the instantaneous average of the 4 circuits' x components, then a plot of the difference of circuit x_1 from the average $d=x_1-\bar{x}$ versus time should be ≈ 0 for synchronized systems. Such a plot is shown for the Rossler-like circuits in Fig. 17. We see that the difference d is not zero and shows large bursts. These bursts are similar in nature to on–off intermittency.[56,92,93] What causes them?

Even though the system is above the Lyapunov exponent threshold c_{sync} we must realize that this exponent is only an ergodic average over the attractor. Hence, if the system has any invariant sets that have stability exponents greater than the Lypunov exponents of the modes, even at couplings above c_{sync}, these invariant sets may still be unstable. When any system wanders near them, the tendency will be for individual systems to diverge by the growth of that mode, which is unstable on the invariant set. This causes the bursts in Fig. 17. We have shown that the bursts can be directly associated with unstable periodic orbits (UPO) in the Rossler-like circuit.[94] These bursts do subside at greater coupling strengths, but even then some deviations can still be seen that may be associated with unstable portions of the attractor that are not invariant sets (e.g., part of an UPO).

The criteria for guaranteed synchronization is still under investigation,[95–97] but the lesson here is that the naive views [(1) and (2) above] that there is a sharp threshold for synchronization and that above that threshold synchronization is guaranteed, are incorrect. The threshold is actually a rather ''fuzzy'' one. It might be best drawn as an (infinite) number of thresholds.[98,99] This is shown in Fig. 18, where a more realistic picture of the stability diagram near the mode 1 threshold is plotted. We see that at a minimum we need to have the coupling be *above* the highest threshold for invariant sets (UPOs and unstable fixed points). A better synchronization criteria, above the invariant sets one, has been suggested by Gauthier *et al.*[97] Their suggestion, for two diffusively coupled systems ($\mathbf{x}^{(1)}$ and $\mathbf{x}^{(2)}$), is to use the criteria $d|\Delta\mathbf{x}|/dt<0$, where $\Delta\mathbf{x}=\mathbf{x}^{(1)}-\mathbf{x}^{(2)}$. A similar suggestion regarding ''monodromy'' in a perturbation decrease was put forward by Kapitaniak.[100] There would be generalizations of this mode analysis for N coupled systems, but these have not been worked out. An interesting approach is taken by Brown,[95] who shows that one can use an averaged Jacobian (that is, averaged over the attractor) to estimate the stability in an optimal fashion. This appears to be less strict than the Gauthier requirement, but more strict than the Lyapunov exponents criterion. Research is still ongoing in this area.[96]

C. Desynchronization thresholds at increased coupling

Let us look at the full stability diagram for modes 1 and 2 for the Rossler-like circuit system when we couple with the x coordinates diffusively, rather than the y's. That is, choose $E_{ij}=0$ for all i and $j=1$, 2,3, except $E_{11}=1$. This is shown in Fig. 19. Note how the mode-2 diagram is just a rescaled mode-1 diagram by a factor of 1/2 in the coupling range. We can now show another, counterintuitive feature that we missed in our naive view. Figure 19 (similar to Fig. 3) shows that the modes go unstable as we *increase* the coupling. The synchronized motion is Lyapunov stable only over a finite range of coupling. Increasing the coupling does not necessarily guarantee synchronization. In fact, if we couple the

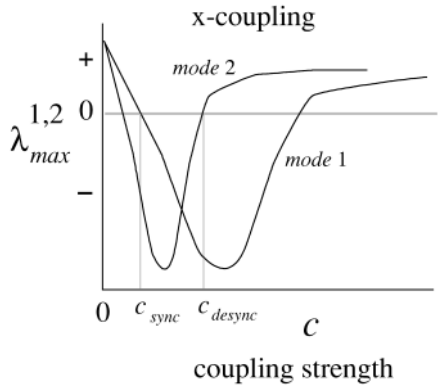

FIG. 19. The stability diagram for modes 1 and 2 for the x-coupled Rössler circuits.

systems by the z variables we will never get synchronization, even when $c=\infty$. The latter case of infinite coupling is just the CR drive response using z. We already know that in that regime both the z and x drivings do not cause synchronization in the Rossler system. We now see why. Coupling through only one component does not guarantee a synchronous state and we have found a counterexample for number (3) in our naive views, that increasing the coupling will guarantee a synchronous state.

Now, let us look more closely at how the synchronous state goes unstable. In finding the c_{sync} threshold we noted that mode 1 was the most unstable and was the last to be stabilized as we increased c. Near c_{desync} we see that the situation is reversed: mode 2 goes unstable first and mode 1 is the most stable. This is also confirmed in the experiment[21] where the four systems go out of synchronization by having, for example, system-1=system-3 and system-2=system-4 while system-1 and system-2 diverge. This is exactly a spatial mode-2 growing perturbation. It continues to rather large differences between the systems with mode-1 perturbations remaining at zero, i.e., we retain the system-1=system-3 and system-2=system-4 equalities.

Since for larger systems ($N>4$) the higher mode stability plots will be squeezed further toward the ordinate axis, we may generalize and state that if there exists a c_{desync} upon increasing coupling, then the *highest*-order mode will always go unstable first. We call this a *short-wavelength bifurcation*.[21] It means that the smallest spatial wavelength will be the first to grow above c_{desync}. This is counter to the usual cases, where the longest or intermediate wavelengths go unstable first. What we have in the short-wavelength bifurcation is an extreme form of the Turing bifurcation[101] for chaotic, coupled systems.

Note that this type of bifurcation can happen in any coupled system where each oscillator or node has ''internal dynamics'' that are not coupled *directly* to other nodes. In our experiment, using x coupling, y and z are internal dynamical variables. In biological modeling where cells are coupled through voltages or certain chemical exchanges, but there are internal chemical dynamics, too, the same situation can occur. All that is required is that the uncoupled variables form an unstable subsystem and the coupling can be pushed above c_{desync}. If this were the case for a continuous system (which would be modeled by a PDE), then the short-wavelength bifurcation would produce a growing perturbation that had an infinitesimal wavelength. So far we do not know of any such findings, but they would surely be of interest and worth looking for.

D. Size limits on certain chaotic synchronized arrays

When we consider the cases in which ($N>4$) we come to the following surprising conclusion that counters naive feature (4). Whenever there is desynchronization with increasing coupling there is always an upper limit on the number of systems we can add to the array and still find a range of coupling in which synchronization will take place.

To see this examine Fig. 20, which comes from an $N=16$ Rossler-like circuit system. We see that the scaling laws relating the stability diagrams for the modes eventually squeeze down the highest mode's stability until just as the first mode is becoming stable, the highest mode is going unstable. In other words c_{sync} and c_{desync} cross on the c axis. Above $N=16$ we never have a situation in which all modes are simultaneously stable. In Ref. 21 we refer to this as a *size effect*.

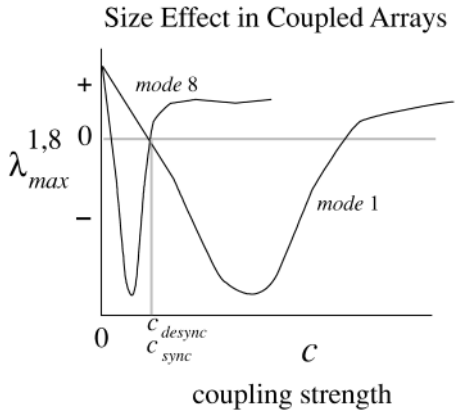

FIG. 20. The stability diagram for 16 x-coupled Rössler circuits showing that all modes cannot be simultaneously stable, leading to a size limit in the number of synchronized oscillators we can couple.

E. Riddled basins of synchronization

There is still one more type of strange behavior in coupled chaotic systems, and this comes from two phenomena. One is the existence of unstable invariant sets (UPOs) in a synchronous chaotic attractor and the other is the simultaneous existence of two attractors, a chaotic synchronized one and another, unsynchronized one. In our experiment these criteria held just below c_{desync}, where we had a synchronous chaotic attractor containing unstable UPOs and we had a periodic attractor (see Fig. 21). In this case, instead of attractor bursting or bubbling, we see what have come to be called *riddled basins*. When the systems burst apart near an UPO, they are pushed off the synchronization manifold. In this case they have another attractor they can go to, the periodic one.

The main feature of this behavior is that the basin of attraction for the periodic attractor is intermingled with the synchronization basin. In fact, the periodic attractor's basin

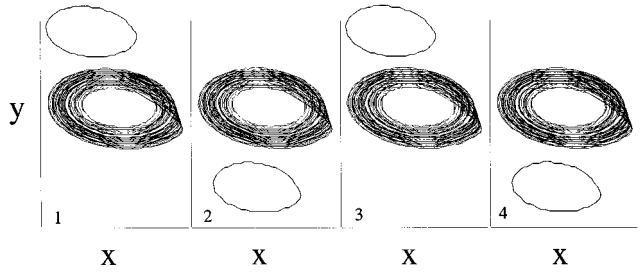

FIG. 21. Simultaneous existence of two attractors in the coupled Rössler.

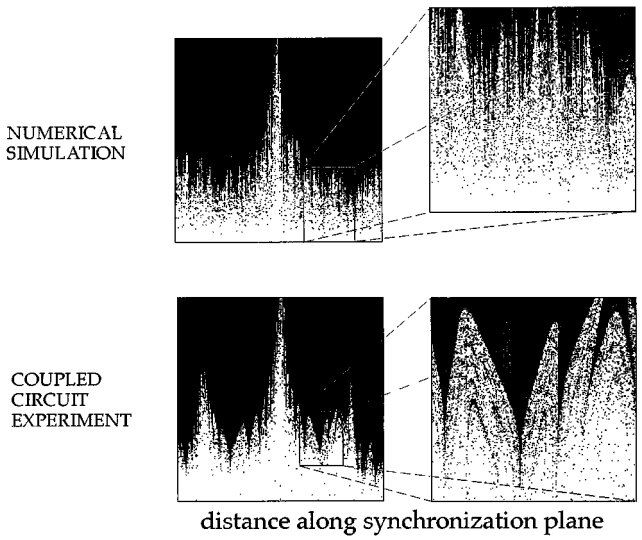

FIG. 22. Simultaneous existence of two attractors in the coupled Rössler.

riddles the synchronized attractor's basin. This was first studied theoretically by Alexander *et al.*[102] and followed by several papers describing the theory of riddled basins.[56,57,98,103–105] Later direct experimental evidence for riddled basins was found by Heagy *et al.*[22] Since then Lai[106] has shown that parameter space can be riddled and others have studied the riddling phenomena in other systems.[107,108]

In our experiment with four coupled, chaotic systems we used a setup that allowed us to examine what might be called a cross section of the riddled basin. We varied initial conditions of the four oscillators so as to produce a 2-D basin map that was consistent with the short-wavelength instability that showed up in the bursts taking the overall system to the other attractor off the synchronization manifold. All z variables were set to the same value for all initial conditions. All four x components were set to the same value that was varied from -3.42 to 6.58. A new variable u representing the mode-2 perturbation was varied from 0.0 to 7.0 for each initial condition and the y variables were set to values that matched the mode-2 wave form: $y_1=y_3=u$ and $y_2=y_4=-u$. The variables x and u made up the 2-D initial condition ''grid'' that was originally suggested by Ott.[109] Varying x changed all the system's x components and kept the systems on the synchronization manifold. Varying u away from zero lifted the systems from the synchronization manifold.

When one of the initial conditions led to a final state of synchronization, it was colored white. When the final state was the periodic, nonsynchronized attractor it was colored black. Figure 22 shows the result of this basin coloring for both the experiment and numerical simulation.[22] The basin of the synchronized state is indeed riddled with points from the basin of the periodic state. The riddling in these systems is extreme in that even infinitesimally close to the synchronization manifold there are points in the basin of the periodic attractor. To put it another way, any open set containing part of the synchronization manifold will *always* contain points from the periodic attractor basin and those points will be of nonzero measure.

Ott *et al.*[57] have shown that near the synchronization manifold the density ρ of the other attractor's basin points will scale as $\rho\sim u^{\alpha}$. In our numerical model we found $\alpha=2.06$ and in the experiment we found $\alpha=2.03$.

The existence of riddled basins means that the final state is uncertain, even more uncertain than where there exist ''normal'' fractal basin boundaries.[110–113]

F. Master stability equation for linearly coupled systems

Recently we have explored synchronization in other coupling schemes. Surprisingly, large classes of coupled-systems problems can be solved by calculating once and for all a stability diagram unique to the oscillators used by using scaling arguments similar to above. In fact, the scaling approach of diffusively coupled systems is a special case of our more general solutions. Although we will be publishing detailed results elsewhere,[114,115] we will outline the approach here and show how the general master stability function so obtained can be used for any linear coupling scheme.

If we start with the particular coupling scheme in Eq. (25) and first decompose the matrix into a diagonal part (with **F** along the diagonal) and second ''factor out'' the **E** matrix that is in all the remaining terms, we get an equation of motion,

$$\frac{d\mathbf{x}}{dt}=\mathbf{F}(\mathbf{x})+c\mathbf{G}\otimes\mathbf{E}\cdot\mathbf{x}, \tag{31}$$

where $\mathbf{F}(\mathbf{x})$ has $\mathbf{F}(\mathbf{x}^{(i)}$ for the ith node block and a variational (stability) equation of the form

$$\frac{d\xi}{dt}=[\mathbf{1}\otimes D\mathbf{F}+c\mathbf{G}\otimes\mathbf{E}]\cdot\xi, \tag{32}$$

where $\mathbf{x}=(\mathbf{x}^{(1)},\mathbf{x}^{(2)},\ldots,\mathbf{x}^{(N)})$, $\mathbf{1}$ is an $N\times N$ unit matrix, $\xi=(\xi^{(1)},\xi^{(2)},\ldots,\xi^{(N)})$ with each $\xi^{(i)}$ a perturbation on the ith node's coordinates $\mathbf{x}^{(i)}$,) and $\mathbf{G}$ is given by

$$\mathbf{G}=\begin{pmatrix} -2 & 1 & 0 & \cdots & 1 \\ 1 & -2 & 1 & \cdots & 0 \\ 0 & 1 & -2 & \cdots & 0 \\ \vdots & \vdots & \vdots & \vdots & \vdots \\ 1 & 0 & \cdots & 1 & -2 \end{pmatrix}. \tag{33}$$

The decomposition and factoring are rigorous since we do the ''multiplication'' with a direct product of matrices ($\otimes$). The **E** matrix operates on individual node components to choose the same combination of dynamical variables from each node and the **G** matrix determines what combination of nodes will feed into each individual node. To obtain the block diagonal variational form of Eq. (25) we have used Fourier modes to diagonalize the node matrix **G**.

We now make the observation that Eq. (31) is the form for *any* linear coupling scheme involving identical nodes in which we use the same linear combination of each node's

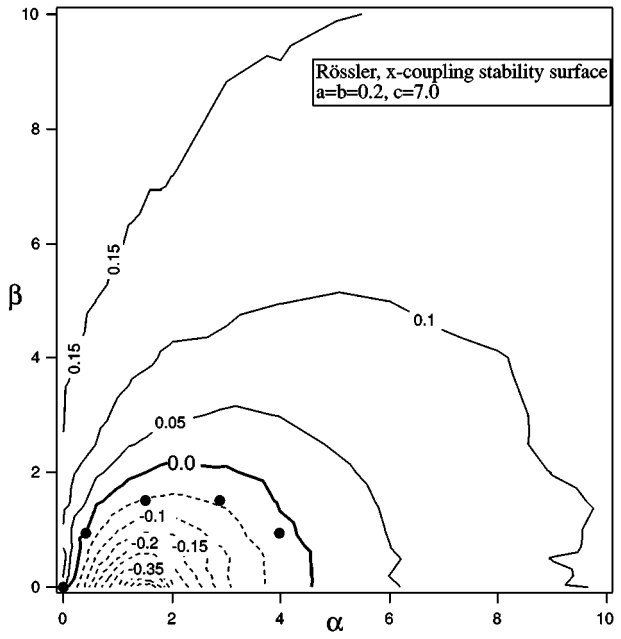

FIG. 23. Contour map of the stability surface for a Rössler oscillator ($a=b=0.2$, $c=7.0$). The dashed lines demark negative (stable) contours and the solid lines demark positive (unstable) contours. The numbered dots show the value of the coupling constant times the eigenvalues for an array of five asymmetrically, diffusively coupled Rössler systems.

variables. Therefore, in diagonalizing **G** we will always reduce the variational problem to an *m*-dimensional ''mode'' equation like

$$\frac{d\xi^{(k)}}{dt}=[D\mathbf{F}+c\gamma_k\mathbf{E}]\cdot\xi^{(k)}, \tag{34}$$

where γ_k is an eigenvalue of **G**.

Now consider making the following stability diagram. Start with the generic variational equation,

$$\frac{d\zeta}{dt}=[D\mathbf{F}+(\alpha+i\beta)\mathbf{E}]\cdot\zeta, \tag{35}$$

and calculate the maximum Lyapunov exponents for all values of α and β. The surface of $\lambda_{\max}$ values over the complex (α,β) plane provides information on the stability for *all* the possible linear couplings (**G**) using the particular local variables selected by **E**, and it gives the master stability function we mentioned above. Hence, given a **G** we diagonalize it (getting, in general, complex eigenvalues γ_k) and for each complex number $c\gamma_k$ we merely examine the $\lambda_{\max}$ surface at $\alpha+i\beta=c\gamma_k$ to see if that eigenmode is stable. In this way, given **E**, we reduce the stability problem to a simple eigenvalue problem for each linear coupling scheme **G**.

We produced such a plot for the Rössler oscillator. This is shown in Fig. 23. If we now want to couple *N* such oscillators using only the *x* components in an asymmetric, cyclic way:

$$\mathbf{E}=\begin{pmatrix}1&0&0\\0&0&0\\0&0&0\end{pmatrix}, \tag{36}$$

$$\frac{dx^{(i)}}{dt}=-(y^{(i)}+z^{(i)})+\sigma(c_1x^{(i+1)}+c_2x^{(i-1)}-2x^{(i)}),$$

where $c_1+c_2=2$, and $i=1,...,N$, we will get complex eigenvalues for **G**: $2\sigma[1-\cos(2\pi k/N)]\pm i2\sigma(1-c_1)\sin(2\pi k/N)$, $k=0,1,...,[[N/2]]$, where $[[\cdot]]$ means integer part of. If we choose a coupling constant of $\sigma=0.55$, **G** components of $c_1=1.4$ and $c_2=0.6$ and $N=5$, we get the dots in Fig. 23. The number on each dot is the mode number. We see by the location of the dots that the synchronous state is just barely stable. Variations in the coupling constants can cause various modes to go unstable. We are presently working on this more general approach and testing it with coupled chaotic circuits. We will report more on this elsewhere.

VI. DETECTION: TIMES SERIES, SYNCHRONIZATION, AND DYNAMICAL INTERDEPENDENCE

A. The general problem: Simultaneous time series

Suppose we had simultaneous time series of all the variables of two dynamical systems (system 1 and system 2) with equal dimension. We could tell if they were in identical synchronization by plotting them in pairs (system 1 variable versus system 2 variable) and seeing if all pairings gave a 45° line. Suppose we suspected that the two systems were not identical, but in some type of general synchronization with each other. For example, we suspect there is a one-to-one, smooth function ϕ relating system 1 to system 2. How could we determine if such a ϕ existed from the data?

In our recent papers[77,78,82] we considered such questions as this. These questions come up quite often when analyzing time series data, for example for determinism, effects of filtering, for synchronization or general synchronization, and correct embedding dimension. What we are asking can be broken down to several simpler questions: is there a function ϕ from system 1 to system 2 that is continuous? Does the inverse of ϕ exist (equivalently, is ϕ^{-1} continuous)? Is ϕ smooth (differentiable)? Is ϕ^{-1} smooth (differentiable)? We showed that one can develop statistics that directly gauge whether two datasets are related by continuous and/or smooth functions. These statistics have proven to be fundamental in that questions about continuity and smoothness come up in different guises very often.

For example, what is the relationship of an attractor reconstructed from a time series to the reconstruction from the same time series passed through a filter? Will both attractors have the same fractal dimension? It is known that filters can change the dimension of an attractor.[81] But it is also known that if the relation between the unfiltered and filtered attractor is continuously differentiable (C^1),[116] then the fractal dimension will not change. In this case it would be useful to have a statistical quantity that could gauge if there existed a $C^1\phi$ that related the reconstructions.

We can also test determinism in time series using continuity statistics. Determinism means that points in phase space close in the present will be close in the future. This just states the continuity property of a deterministic flow. Given pure data, we do not know if there is a flow, so such a

statistic would be useful. The inverse continuity and smoothness conditions can tell us if the flow is invertible and differentiable, respectively.

There are other uses for such statistics. Below we show some simple examples of how we can use them to determine generalized synchronization situations.

B. The statistics: Continuity and differentiability

We give a short introduction on how to develop our statistics. We refer the reader to more detailed derivations in the literature.[77,78,82] Below we assume we are working on multivariate data in two spaces X and Y, not necessarily of the same dimension. Simultaneous reconstruction of two attractors from datasets as mentioned above is an example of such a situation. In such reconstructions individual points in X and Y are associated simply by virtue of being measured at the same time. We call this association $f:X\rightarrow Y$. We ask, given the data, when can we be convinced that f is continuous? That f^{-1} is continuous? That f is differentiable?

We start with the continuity statistic. The definition of continuity is, the function f is continuous at a point $\mathbf{x}_0 \in X$ if $\forall > 0 \exists \delta > 0$ such that $\|\mathbf{x}-\mathbf{x}_0\| < \delta \Rightarrow \|f(\mathbf{x})-f(\mathbf{x}_0)\| < \epsilon$. In simpler terms, if we restrict ourselves to some local region around $f(\mathbf{x}_0) \in Y$, then there must exist a local region around $\mathbf{x}_0$ *all* of whose points are mapped into the $f(\mathbf{x}_0)$ region. We choose an ϵ-sized set around the fiducial point $\mathbf{y}_0$, we also choose a δ-sized set around its pre-image $\mathbf{x}_0$. We check whether all the points in the δ set map *into* the ϵ set. If not, we reduce δ and try again. We continue until we run out of points or all points from a small-enough δ set fall in the ϵ set. We count the number of points in the ϵ set (n_ϵ) and the δ set (n_δ). We do not include the fiducial points $\mathbf{y}_0$ or $\mathbf{x}_0$, since they are present by construction. Generally $n_\epsilon \geqslant n_\delta$, since points other than those near $\mathbf{x}_0$ can also get mapped to the ϵ set, but this does not affect continuity.

We now choose a null hypothesis that helps us generate a probability that one should find n_ϵ and n_δ points in such an arrangement. We choose the simplest, namely, that placements of the points on the $\mathbf{x}$ and $\mathbf{y}$ attractors are independent of each other. This null hypothesis is not trivial. It is typical of what one would like to disprove early on in any attractor analysis, namely that the data have a relation to each other.

Given the null hypothesis we approximate the probability of a point from the δ set falling at random in the ϵ set as $p=n_\epsilon/N$, where N is the total number of points on the attractor. Then the probability that n_δ points will fall in the ϵ set is p^{n_δ}. We obtain a likelihood that this will happen by taking the ratio of this probability to the probability for the most likely event, p_{binmax}. The latter is just the maximum of the binomial distribution for n_δ points given probability p for each individual event. We see that p^{n_δ} is simply the ''tail end'' of the binomial distribution. The maximum generally will occur for some intermediate number of δ points, say $m(<n_\delta)$, falling in the ϵ set. If $p^{n_\delta} \ll p_{\text{binmax}}$, then the null hypothesis is not likely and can be rejected.

We define the continuity statistic as $\Theta_C 0 = 1 - p^{n_\delta}/p_{\text{binmax}}$. When $\Theta_C 0 \approx 1$, we can confidently reject the null hypothesis. The points in the ϵ set are behaving as though they are generated by a continuous function on the δ set. When $\Theta_C 0 \approx 0$ we cannot reject the null hypothesis and the points are behaving as though they are independent. Note that if we run out of points ($n_\delta = 0$), then we usually take the logical position that we cannot reject the null hypothesis and set $\Theta_C 0 = 0$. $\Theta_C 0$ will depend on ϵ, the resolution, and we will examine the statistic for a range of ϵ's. To get a global estimate of the continuity of f on the attractor we average $\Theta_C 0$ over the entire attractor or over a random sampling of points on it. We present those averages here. For testing the inverse map (ϕ^{-1}) continuity we just reverse the roles of X and Y and δ and ϵ. This give us a statistic $\Theta_I 0$, which gives evidence of the continuity of ϕ^{-1}.

The differentiability statistic is generated in the same vein as the continuity statistic. We start with the mathematical definition of a derivative and apply it locally to the two reconstructions. The generation of the linear map that approximates the derivative and the likelihood estimate associ-

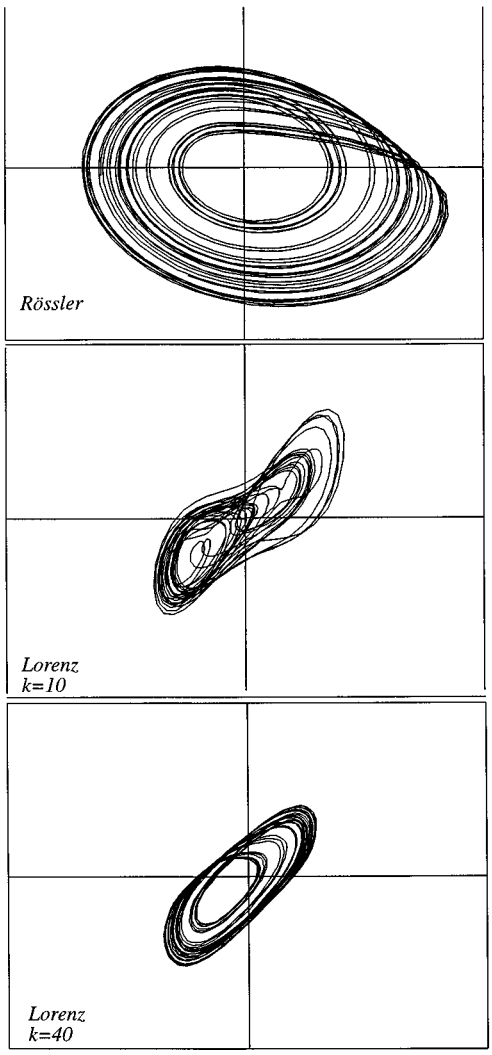

FIG. 24. (a) Rössler and (b) and (c) Lorenz attractors when the Rössler is driving the Lorenz through a diffusive coupling for two different coupling values.

ated with it are more complex than for continuity.

The definition of a derivative at a point $\mathbf{x}_0$ is that a linear operator A exists such that $\forall \epsilon > 0 \exists \delta > 0$ for which $\|\mathbf{x}-\mathbf{x}_0\| < \delta \Rightarrow \|f(\mathbf{x}_0)+A(\mathbf{x}-\mathbf{x}_0)-f(\mathbf{x})\| < \epsilon \|\mathbf{x}-\mathbf{x}_0\|$. This means that there is a linear map that approximates the function at nearby points with an error ϵ in the approximation that is proportional to the distance between those points. Note that ϵ serves a purpose here different from continuity.

The algorithm that we generate from this definition is to first choose an ϵ (error bound) and a δ. Then we find all the points in the local δ set $\{\mathbf{x}_i\}$ and their $\mathbf{y}$ counterparts $\{\mathbf{y}_1\} \in Y$. We approximate the linear operator A as the least squares solution of the linear equations $A(\mathbf{x}_i-\mathbf{x}_0)=(\mathbf{y}_i-\mathbf{y}_0)$. The solution is accomplished by singular value decomposition (SVD).[77] We check if $\|\mathbf{y}_i-\mathbf{y}_0-A(\mathbf{x}_i-\mathbf{x}_0)\| < \epsilon\|\mathbf{x}-\mathbf{x}_0\|$. If not, we decrease δ and try again with fewer, but nearer points. We continue this until we have success or we run out of points.

We choose the null hypothesis that the two sets of vectors $\{\mathbf{x}_i\}$ and $\{\mathbf{y}_i\}$ have zero correlation. We show[77] that this generates a likelihood that any two such sets will give the operator A ''by accident'' as $e^{(1/2)(n_\delta - r_x)(n_\delta - r_y)r^2 d}$, where r^2 is the usual multivariate statistical correlation between $\{\mathbf{x}_i\}$ and $\{\mathbf{y}_i\}$, $d=\min(r_x,r_y)$, and r_x, r_y are the ranks of the $\mathbf{x}$ and $\mathbf{y}$ spaces that come out of the SVD.[77] This is an asymptotic formula. The differentiability statistic $\Theta_C 1$ is given by one minus this likelihood. When $\Theta_C 1 \approx 1$ we can reject the possibility that the points are accidentally related by a linear operator, a derivative. When $\Theta_C 1 \approx 0$, we cannot reject the null hypothesis. As before, when we shrink δ so small that no points other than $\mathbf{x}_0$ remain, we set $\Theta_C 1 = 0$. Analogous to $\Theta_C 0$, the statistic $\Theta_C 1$ depends on ϵ. We typically calculate $\Theta_C 1$ for a range of ϵ's and average over the attractor or over a random sampling of points on it. Similar to the continuity situation we can test the differentiability of ϕ^{-1} by reversing X and Y and δ and ϵ roles. We call this statistic $\Theta_I 1$.

C. Generalized synchronization

We examine the generalized synchronization situation when we have a Rössler system driving a Lorenz system through a diffusive coupling with coupling constant k:

$$\begin{aligned} \dot{x} &= -(y+z), & \dot{u} &= -\sigma u + \sigma v, \\ \dot{y} &= x + a y, & \dot{v} &= -uw + ru - v + k(y-v), \\ \dot{x} &= b + z(x-c), & \dot{w} &= uv - gw, \\ &\text{Rössler} & &\text{Lorenz}, \end{aligned} \tag{37}$$

where $a=b=0.2$, $c=9.0$, $\sigma=10$, $r=60$, and $g=8/3$. Figure 24 shows the Rössler attractor and two Lorenz attractors at $k=10$ and $k=40$. It appears impossible to tell what the relation is between the Rössler and two Lorenz attractors. However, the statistics indicate an interesting relationship.

At lower coupling ($k=10$) there appears to be no function ϕ mapping the Rössler system into the Lorenz. Both the continuity statistic ($\Theta_C 0$) and the differentiability statistic ($\Theta_C 1$) are low, as shown in Fig. 25. But at $k=40$ the continuity statistic approaches 1.0 even for small ϵ sets. That means that we can be confident that the relation between the Rössler and Lorenz is continuous for continuities above $\epsilon = 0.01$, which is shown in Figs. 24(b) and 24(c). This is a small set. On the other hand, the differentiability statistic never gets very high and falls off to zero rather quickly. This implies that at $k=40$ we have a functional relation between the drive and response that is C^0, but not C^1. It turns out that the response is most stable at $k=40$ and increasing the coupling beyond that point will not improve the properties of ϕ. This means that the fractal dimension of the entire Rössler–Lorenz attractor is larger than that of the Rössler itself. Points nearby on the Rössler are related to points nearby on the Lorenz, but not in a smooth fashion.

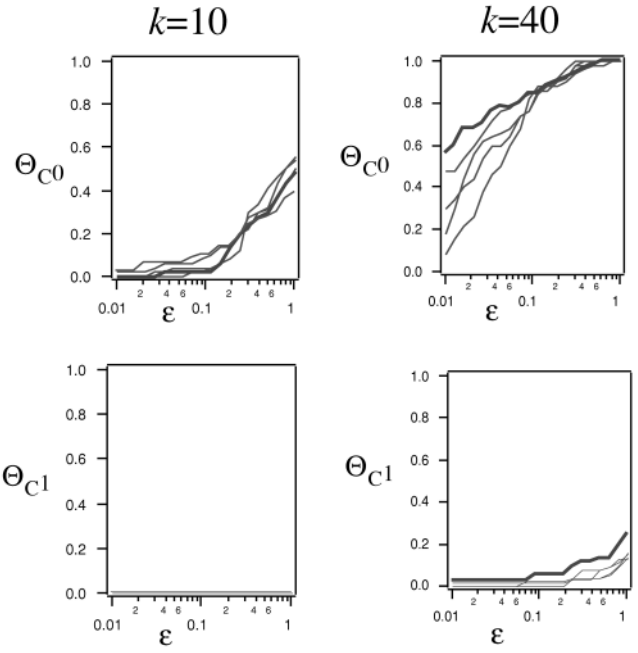

FIG. 25. Continuity and differentiability statistics for a possible functional relation ϕ: Rössler→Lorenz. The statistics were calculated for various number of points on the attractors (16, 32, 64, and 128 K). All ϵ values are scaled to the standard deviation of the attractors.

C. Dynamical interdependence

We see that to show synchronization we need to have access to all the variables' time series. Can we say anything about two simultaneously measured scalar time series and their corresponding reconstructed attractors? The answer is, yes, and it provides information that would be useful in many experimental situations.

Our scenario is that we have an experiment in which we have two (or more) probes at spatially separate points producing dynamical signals that we are sampling and storing as two, simultaneous time series. We use each to reconstruct an attractor. If the signals came from independent dynamical systems, we would expect generically no relationship between them so that the statistics $\Theta_C 0$ and $\Theta_C 1$ and their inverse versions would be low (near zero). However, if they came from the same system, by Taken's theorem each attrac-

tor would be related by a diffeomorphism to the original system's phase space attractor. Since a relationship by diffeomorphism is transitive (i.e., if A is diffeomorphic to B and B is diffeomorphic to C, then A is diffeomorphic to C). The reconstructions would be diffeomorphic. We can use our statistics to test for this.

We can calculate $\Theta_C 0$, $\Theta_C 1$, $\Theta_I 0$, and $\Theta_I 1$ for the two attractors. If they are all near 1.0 for small ϵ values, we have evidence that the two reconstructions are diffeomorphically related. Since the odds for this happening by chance to independent dynamical systems must be small, we make the conclusion that our two time series were sampled from different parts of the same dynamical system—we now have a test for *dynamical interdependence*. For example, we might sample simultaneously the x and y components of the Lorenz system.

An interesting use of this test for dynamical interdependence was done by Schiff *et al.* in an EEG time series.[117] They showed that statistics similar to $\Theta_C 0$ could be developed in which each point would be compared to forward-time-shifted points on the other attractor. This mixes in prediction (determinism) with direct, point-to-point continuity and differentiability. Their results show that dynamical interdependence could be seen where standard statistical tests (e.g., linear correlations) showed no relationships.

Finally, we note that these statistics would also be useful in numerical work since we cannot always have a closed form functional relationship. In the example of the Rössler-driven Lorenz we did not have access to a function ϕ: Rössler→Lorenz, but we could generate the time series for all variables. We could then test for evidence of functional relationships. Such evidence could guide rigorous attempts to prove or disprove the existence of properties of such a function.

[1] J.-C. Roux, R. H. Simoyi, and H. L. Swinney, ''Observation of a strange attractor,'' Physica D **8**, 257–266 (1983).
[2] T. Yamada and H. Fujisaka, ''Stability theory of synchronized motion in coupled-oscillator systems. II,'' Prog. Theor. Phys. **70**, 1240 (1983).
[3] T. Yamada and H. Fujisaka, ''Stability theory of synchronized motion in coupled-oscillator systems. III,'' Prog. Theor. Phys. **72**, 885 (1984).
[4] V. S. Afraimovich, N. N. Verichev, and M. I. Rabinovich, ''Stochastic synchronization of oscillations in dissipative systems,'' Inv. VUZ Rasiofiz. RPQAEC **29**, 795–803 (1986).
[5] T. L. Carroll and L. M. Pecora, ''Synchronizing chaotic circuits,'' IEEE Trans. CAS **38**, 453 (1991).
[6] T. L. Carroll and L. M. Pecora, ''Cascading synchronized chaotic systems,'' Physica D **67**, 126–140 (1993).
[7] T. L. Carroll and L. M. Pecora, ''Synchronizing nonautonomous chaotic circuits,'' IEEE Trans. Circuits Syst. **40**, 646 (1995).
[8] L. M. Pecora and T. L. Carroll, ''Synchronization in chaotic systems,'' Phys. Rev. Lett. **64**, 821 (1990).
[9] L. M. Pecora and T. L. Carroll, ''Driving systems with chaotic signals,'' Phys. Rev. A **44**, 2374 (1991).
[10] J. F. Heagy, T. L. Carroll, and L. M. Pecora, ''Synchronous chaos in coupled oscillator systems,'' Phys. Rev. E **50**, 1874 (1994).
[11] C. Tresser, P. A. Worfolk, and H. Bass, ''Master-slave synchronization from the point of view of global dynamics,'' Chaos **5**, 693 (1995).
[12] L. M. Pecora and T. L. Carroll, ''Pseudoperiodic driving: Eliminating multiple domains of attraction using chaos,'' Phys. Rev. Lett. **67**, 945 (1991).
[13] L. Pecora and T. Carroll, ''Synchronized chaotic signals and systems,'' *SPIE 1992 Proceedings*, San Diego CA (SPIE—The International Society for Optical Engineering, Bellingham, WA, 1992), Vol. 1771, p. 389.
[14] E. N. Lorenz, ''The local structure of a chaotic attractor in pour dimensions,'' Physica D **13**, 90 (1984).
[15] N. F. Rul'kov, A. R. Volkovskii, A. Rodriguez-Lozano *et al.*, ''Mutual synchronization of chaotic self-oscillators with dissipative coupling,'' Int. J. Bifurcation Chaos Appl. Sci. Eng. **2**, 669–676 (1992).
[16] M. Rabinovich (private communication).
[17] V. S. Anishchenko, T. E. Vadivasova, D. E. Posnov *et al.*, ''Forced and mutual synchronization of chaos,'' Sov. J. Commun. Technol. Electron. **36**, 23 (1991).
[18] M. Ding and E. Ott, ''Enhancing synchronism of chaotic systems,'' Phys. Rev. E **49**, R945 (1994).
[19] K. Pyragas, ''Predictable chaos in slightly perturbed unpredictable chaotic systems,'' Phys. Lett. A **181**, 203 (1993).
[20] C. W. Wu and L. O. Chua, ''A unified framework for synchronization and control of dynamical systems,'' Int. J. Bifurcations Chaos **4**, 979 (1994).
[21] J. F. Heagy, L. M. Pecora, and T. L. Carroll, ''Short wavelength bifurcations and size instabilities in coupled oscillator systems,'' Phys. Rev. Lett. **74**, 4185 (1994).
[22] J. F. Heagy, T. L. Carroll, and L. M. Pecora, ''Experimental and numerical evidence for riddled basins in coupled chaotic oscillators,'' Phys. Rev. Lett. **73**, 3528 (1995).
[23] K. Ogata, *Control Engineering* (Prentice–Hall, Englewood Cliffs, NJ, 1990).
[24] R. W. Newcomb and N. El-Leithy, ''Chaos generation using binary hysteresis,'' Circuits Syst. Signal Process. **5**, 321 (1986).
[25] A. Tamasevicius, G. Mykolaitis, A. Cenys *et al.*, ''Synchronization of 4D hyperchaotic oscillators,'' Electron. Lett. **32**, 1536–1537 (1996).
[26] T. Carroll, ''A simple circuit for demonstrating regular and synchronized chaos,'' Am. J. Phys. **63**, 377 (1995).
[27] K. Cuomo and A. V. Oppenheim, ''Circuit implementation of synchronized chaos with applications to communications,'' Phys. Rev. Lett. **71**, 65 (1993).
[28] K. M. Cuomo, A. V. Oppenheim, and S. H. Strogatz, ''Synchronization of Lorenz-based chaotic circuits with applications to communications,'' IEEE Trans. Circuits Syst. **40**, 626–633 (1993).
[29] Lj. Kocarev, K. S. Halle, K. Eckert *et al.*, ''Experimental demonstration of secure communications via chaotic synchronization,'' Int. J. Bifurcations Chaos **2**, 709–713 (1992).
[30] K. Murali and M. Lakshmanan, ''Transmission of signals by synchronization in a chaotic Van der Pol–Duffing oscillator,'' Phys. Rev. E **48**, R1624 (1993).
[31] U. Parlitz, L. O. Chua, L. Kocarev *et al.*, ''Transmission of digital signals by chaotic synchronization,'' Int. J. Bifurcations Chaos **2**, 973–977 (1992).
[32] R. H. Sherman and J. Gullicksen, ''Chaotic communications in the presence of noise,'' *SPIE Conference on Chaos in Communications Proceedings* (SPIE, Bellingham, WA, 1993), Vol. 2038, pp. 141–152.
[33] G. Pérez and H. A. Cerderia, ''Extracting messages masked by chaos,'' Phys. Rev. Lett. **74**, 1970 (1995).
[34] K. M. Short, ''Steps toward unmasking secure communications,'' Int. J. Bifurcations Chaos **4**, 959 (1994).
[35] A. H. MacDonals and M. Plischke, ''Study of the driven damped pendulum: Application to Josephson Junctions and charge-density-wave systems,'' Phys. Rev. B **27**, 201 (1983).
[36] E. Brauer, S. Blochwitz, and H. Beige, ''Periodic windows inside chaos—Experiment versus theory,'' Int. J. Bifurcation Chaos **4**, 1031–1039 (1993).
[37] S. Tankara, T. Matsumoto, and L. O. Chua, ''Bifurcation scenario in a driven R-L-diode circuit,'' Physica D **28**, 317–344 (1987).
[38] C. Grebogi, E. Ott, and J. A. Yorke, ''Attractors on an n-torus: Quasiperiodicity versus chaos,'' Physica D **15**, 354–373 (1985).
[39] D. D'Humieres, M. R. Beasley, B. A. Huberman *et al.*, ''Chaotic states and routes to chaos in the forced pendulum,'' Phys. Rev. A **26**, 3483 (1982).
[40] J. Guemez, M. A. Matas *et al.*, ''Modified method for synchronizing and cascading chaotic systems,'' Phys. Rev. E **52**, 2145 (1995).
[41] R. E. Amritkar and Neelima Gupte, ''Synchronization of chaotic orbits: The effect of a finite time step,'' Phys. Rev. E **47**, 3889 (1993).
[42] T. Stojanovski, L. Kocarev, and U. Parlitz, ''Driving and synchronizing by chaotic impulses,'' Phys. Rev. E **54**, 2128–2131 (1996).

[43] T. Stojanovski, L. Kocarev, Urlich Parlitz *et al.*, ''Sporadic driving of dynamical systems,'' Phys. Rev. E **55**, 4035 (1997).
[44] T. L. Carroll, ''Synchronizing chaotic systems using filtered signals,'' Phys. Rev. E **50**, 2580–2587 (1994).
[45] T. L. Carroll, ''Communicating with use of filtered, synchronized chaotic signals,'' IEEE Trans. Circuits Syst. **42**, 105 (1995).
[46] L. Kocarev and U. Parlitz, ''General approach for chaotic synchronization with applications to communication,'' Phys. Rev. Lett. **74**, 5028 (1995).
[47] T. L. Carroll, J. F. Heagy, and L. M. Pecora, ''Transforming signals with chaotic synchronization,'' Phys. Rev. E **54**(5), 4676 (1996).
[48] W. L. Brogan, *Modern Control Theory* (Prentice–Hall, Englewood Cliffs, NJ, 1991).
[49] M. di Bernardo, ''An adaptive approach to the control and synchronization of continuous-time chaotic systems,'' Int. J. Bifurcations Chaos **6**, 557–568 (1996).
[50] M. di Bernardo, ''A purely adaptive controller to synchronize and control chaotic systems,'' Phys. Lett. A **214**, 139 (1996).
[51] C.-C. Chen, ''Direct chaotic dynamics to any desired orbits via a closed-loop control,'' Phys. Lett. A **213**, 148 (1996).
[52] G. Chen and D. Lai, ''Feedback control of Lyapunov exponents for discrete-time dynamical systems,'' Int. J. Bifurcations Chaos **6**, 1341 (1996).
[53] J. H. Peng, E. J. Ding, M. Ding *et al.*, ''Synchronizing hyperchaos with a scalar transmitted signal,'' Phys. Rev. Lett. **76**, 904–907 (1996).
[54] L. S. Tsimring and M. M. Sushchik, ''Multiplexing chaotic signals using synchronization,'' Phys. Lett. **213B**, 155–166 (1996).
[55] A. Cenys, A. Namajunas, A. Tamasevicius *et al.*, ''On–off intermittency in chaotic synchronization experiment,'' Phys. Lett. A **213**, 259 (1996).
[56] E. Ott and J. C. Sommerer, ''Blowout bifurcations: The occurrence of riddled basins and on–off intermittency,'' Phys. Lett. A **188**, 39–47 (1994).
[57] E. Ott, J. C. Sommerer, J. C. Alexander *et al.*, ''Scaling behavior of chaotic systems with riddled basins,'' Phys. Rev. Lett. **71**, 4134 (1993).
[58] F. Moon, *Chaotic Vibrations* (Wiley, New York, 1987).
[59] P. So, E. Ott, and W. P. Dayawansa, ''Observing chaos: Deducing and tracking the state of a chaotic system from limited observation,'' Phys. Lett. A **176**, 421 (1993).
[60] E. Ott, C. Grebogi, and J. A. Yorke, ''Controlling a chaotic system,'' Phys. Rev. Lett. **64**, 1196 (1990).
[61] R. Brown and P. Bryant, ''Computing the Lyapunov spectrum of a dynamical system from an observed time series,'' Phys. Rev. A **43**, 2787 (1991).
[62] R. Brown, ''Calculating Lyapunov exponents for short and/or noisy data sets,'' Phys. Rev. E **47**, 3962 (1993).
[63] R. Brown, N. F. Rul'kov, and N. B. Tufillaro, ''The effects of additive noise and drift in the dynamics of the driving on chaotic synchronization,'' preprint, 1994.
[64] R. Brown, N. F. Rul'kov, and N. B. Tufillaro, ''Synchronization of chaotic systems. The effects of additive noise and drift in the dynamics of the driving,'' preprint, 1994.
[65] U. Parlitz, ''Estimating model parameters from time series by autosynchronization,'' Phys. Rev. Lett. **76**, 1232 (1996).
[66] J. F. Heagy and T. L. Carroll, ''Chaotic synchronization in Hamiltonian systems,'' Chaos **4**, 385–390 (1994).
[67] T. L. Carroll and L. M. Pecora, ''Synchronizing hyperchaotic volume-preserving map circuits,'' IEEE Trans. Circuits Syst. (in press).
[68] A. J. Lichtenberg and M. A. Lieberman, *Regular and Stochastic Motion* (Springer-Verlag, New York, 1983).
[69] L. M. Pecora and T. L. Carroll, ''Volume-preserving and volume expanding, synchronized chaotic systems,'' Phys. Rev. E (in press).
[70] L. Kocarev, ''Chaos synchronization of high-dimensional dynamical systems,'' IEEE Trans. Circuits Syst. **42**, 1009–1012 (1995).
[71] L. Kocarev, U. Parlitz, and T. Stojanovski, ''An application of synchronized chaotic dynamic arrays,'' Phys. Lett. A **217**, 280–284 (1996).
[72] R. Roy and K. Scott Thornburg Jr., ''Experimental synchronization of chaotic lasers,'' Phys. Rev. Lett. **72**, 2009 (1994).
[73] P. Colet and R. Roy, ''Digital communication with synchronized chaotic lasers,'' Opt. Lett. **19**, 2056 (1994).
[74] P. M. Alsing, A. Gavrielides, V. Kovanis *et al.*, ''Encoding and decoding messages with chaotic lasers,'' Phys. Rev. E (in press).
[75] D. W. Peterman, M. Ye, and P. E. Wigen, ''High frequency synchronization of chaos,'' Phys. Rev. Lett. **74**, 1740 (1995).
[76] N. Rul'kov, M. M. Sushchik, L. S. Tsimring *et al.*, ''Generalized synchronization of chaos in directionally coupled chaotic systems,'' Phys. Rev. E **51**, 980 (1995).
[77] L. Pecora, T. Carroll, and J. Heagy, ''Statistics for mathematical properties of maps between time-series embeddings,'' Phys. Rev. E **52**, 3420 (1995).
[78] L. M. Pecora, T. L. Carroll, and J. F. Heagy, ''Statistics for continuity and differentiability: An application to attractor reconstruction from time series,'' in *Nonlinear Dynamics and Time Series: Building a Bridge Between the Natural and Statistical Sciences, Fields Institute Communications*, edited by C. D. Cutler and D. T. Kaplan (American Mathematical Society, Providence, RI, 1996), Vol. 11, pp. 49–62.
[79] H. D. I. Abarbanel, N. F. Rulkov, and M. M. Sushchik, ''Generalized synchronization of chaos: The auxiliary system approach,'' Phys. Rev. E **53**, 4528 (1996).
[80] L. Kocarev and U. Parlitz, ''Generalized synchronization, predictability and equivalence of unidirectionally coupled systems,'' Phys. Rev. Lett. **76**, 1816–1819 (1996).
[81] R. Badii, G. Broggi, B. Derighetti *et al.*, ''Dimension Increase in Filtered Chaotic Signals,'' Phys. Rev. Lett. **60**, 979 (1988).
[82] L. Pecora and T. Carroll, ''Discontinuous and nondifferentiable functions and dimension increase induced by filtering chaotic data,'' Chaos **6**, 432–439 (1996).
[83] K. M. Campbell and M. E. Davies, ''The existence of inertial functions in skew product systems,'' Nonlinearity **9**, 801–817 (1996).
[84] M. E. Davies and K. M. Campbell, ''Linear recursive filters and nonlinear dynamics,'' Nonlinearity **9**, 487–499 (1996).
[85] D. S. Broomhead, J. P. Huke, G. D. de Villiers *et al.*, Report No. Appendix 10, Final Report to SRP, Assignment No. AS02 BP20, 1994.
[86] J. Stark and M. E. Davies, ''Recursive filters driven by chaotic signals,'' IEE Digest **143**, 1–16 (1994).
[87] J. Stark (private communication).
[88] B. Hunt, E. Ott, and J. A. Yorke, ''Differentiable generalized synchronization of chaos,'' Phys. Rev. E **55**, 4029 (1997).
[89] B. R. Hunt, E. Ott, and J. A. York, ''Fractal dimensions of chaotic saddles of dynamical systems,'' Phys. Rev. E **54**(5), 4819 (1996).
[90] J. Stark, ''Invariant graphs for forced systems,'' Physica D (in press).
[91] B. Hunt (private communication).
[92] J. F. Heagy, N. Platt, and S. M. Hammel, ''Characterization of on–off intermittency,'' Phys. Rev. E **49**, 1140 (1994).
[93] N. Platt, S. M. Hammel, and J. F. Heagy, ''Effects of additive noise on on–off intermittency,'' Phys. Rev. Lett. **72**, 3498 (1994).
[94] J. F. Heagy, T. L. Carroll, and L. M. Pecora, ''Desynchronization by periodic orbits,'' Phys. Rev. E **52**, R1253 (1995).
[95] R. Brown, ''Synchronization of chaotic systems: Transverse stability of trajectories in invariant manifolds,'' Chaos **7**, 395 (1997).
[96] L. M. Pecora, T. L. Carroll, D. J. Gauthier *et al.*, ''Criteria which guarantee synchronization in coupled, chaotic systems'' (in preparation).
[97] D. J. Gauthier and J. C. Bienfang, ''Intermittent loss of synchronization in coupled chaotic oscillators: Toward a new criterion for high-quality synchronization,'' Phys. Rev. Lett. **77**, 1751 (1996).
[98] P. Ashwin, J. Buescu, and I. Stewart, ''From attractor to chaotic saddle: A tale of transverse instability,'' Nonlinearity **9**, 703–737 (1994).
[99] S. C. Venkataramani, B. Hunt, and E. Ott, ''The bubbling transition,'' Phys. Rev. E **54**, 1346–1360 (1996).
[100] T. Kapitaniak, ''Monotone synchronization of chaos,'' Int. J. Bifurcations Chaos **6**, 211 (1996).
[101] A. Turing, Philos. Trans. B **237**, 37 (1952).
[102] J. C. Alexander, J. A. Yorke, Z. You *et al.*, ''Riddled basins,'' Int. J. Bifurcations Chaos **2**, 795 (1992).
[103] I. Kan, ''Open sets of diffeomorphisms having two attractors, each with an everywhere dense basin,'' Bull. Am. Math. Soc. **31**, 68 (1994).
[104] E. Ott, J. C. Alexander, I. Kan *et al.*, ''The transition to chaotic attractors with riddled basins,'' Physica D (in press).
[105] J. C. Sommerer and E. Ott, ''A physical system with qualitatively uncertain dynamics,'' Nature (London) **365**, 138–140 (1993).
[106] Y-C. Lai and R. L. Winslow, ''Riddled parameter space in spatiotemporal chaotic dynamical systems,'' Phys. Rev. Lett. **72**, 1640 (1994).
[107] R. H. Parmenter and L. Y. Yu, ''Riddled behavior of certain synchronized systems,'' Phys. Lett. A **189**, 181–186 (1994).
[108] P. Ashwin, J. Buescu, and I. Stewart, ''Bubbling of attractors and synchronization of chaotic oscillators,'' Phys. Lett. A **193**, 126–139 (1994).
[109] E. Ott (private communication).
[110] C. Grebogi, E. Ott, and J. A. Yorke, ''Crises, sudden changes in chaotic

attractors and transient chaos,'' Physica D **7**, 181 (1983).
[111] T. L. Carroll, L. M. Pecora, and F. J. Rachford, ''Chaotic transients and multiple attractors in spin-wave experiments,'' Phys. Rev. Lett. **59**, 2891 (1987).
[112] S. W. McDonald, C. Grebogi, E. Ott *et al.*, ''Fractal basin boundaries,'' Physica D **17**, 125 (1985).
[113] B.-S. Park, C. Grebogi, E. Ott *et al.*, ''Scaling of fractal basin boundaries near intermittency transitions to chaos,'' Phys. Rev. A **40**, 1576 (1989).
[114] L. M. Pecora, ''Synchronization conditions and desynchronizing patterns in coupled limit-cycle and chaotic systems,'' in preparation.
[115] L. M. Pecora, T. L. Carroll, G. Johnson *et al.*, ''Master stability function for synchronized coupled systems,'' in preparation.
[116] T. Sauer and J. A. Yorke, ''Are the dimensions of a set and its image equal under typical smooth functions?,'' Ergodic Theory Dyn. Syst. (in press).
[117] S. Schiff, P. So, T. Chang *et al.*, ''Detecting dynamical interdependence and generalized synchrony through mutual prediction in a neural ensemble,'' Phys. Rev. E **54**, 6708–6724 (1996).